



รายงานวิจัยฉบับสมบูรณ์

โครงการ การวิเคราะห์พฤติกรรมการถ่ายเทความร้อนในช่องวัสดุพรุนที่ได้รับพลังงาน ความร้อนจากคลื่นร้อนจากคลื่นไมโครเวฟโดยใช้ท่อนำคลื่นทรงสี่เหลี่ยม (เชิงทฤษฎี และการทดลอง)

โดย ผู้ช่วยศาสตราจารย์ ดร. วาทิต ภักดี และคณะ

รายงานวิจัยฉบับสมบูรณ์

โครงการ การวิเคราะห์พฤติกรรมการถ่ายเทความร้อนในช่องวัสดุพรุนที่ได้รับพลังงาน ความร้อนจากคลื่นร้อนจากคลื่นไมโครเวฟโดยใช้ท่อนำคลื่นทรงสี่เหลี่ยม (เชิงทฤษฎี และการทดลอง)

คณะผู้วิจัย

- 1) ผู้ช่วยศาสตราจารย์ ดร. วาทิต ภักดี
- 2) รองศาสตราจารย์ ดร. ผดุงศักดิ์ รัตนเดโช

สังกัด

คณะวิศวกรรมศาสตร์ ม. ธรรมศาสตร์ คณะวิศวกรรมศาสตร์ ม. ธรรมศาสตร์

สนับสนุนโดยสำนักงานคณะกรรมการอุตมศึกษา และสำนักงานกองทุนสนับสนุนการวิจัย (ความเห็นในรายงานนี้เป็นของผู้วิจัย สกอ. และ สกว. ไม่จำเป็นต้องเห็นด้วยเสมอไป)

บทคัดย่อ

งานวิจัยนี้ศึกษากระบวนการถ่ายเทความร้อนในวัสดุพรุนอิ่มตัว ซึ่งแบ่งได้เป็น 2 ส่วนที่เกี่ยวข้อง กัน ส่วนแรกศึกษาการถ่ายเทความร้อนในวัสดุพรุนที่ได้รับความร้อนหรือความเย็นแบบส่วนโดยการ พาความร้อน แบบจำลองทางคณิตศาสตร์ในรูปของชุดสมการถูกพัฒนาขึ้นโดยอาศัยดัวแบบที่มีชื่อ ว่า Brinkmann-extended Darcy ผลเฉลยของชุดของสมการกำกับนี้หาได้จากการใช้ระเบียบวิธี finite difference ภายใต้เงื่อนไขขอบเขตที่เหมาะสม การพาความร้อนที่ในวัสดุพรุนไม่เพียงแต่เกิด จากเกรเดียนท์ของความหนาแน่นที่มีค่าลบในทิศทางแรงโน้มถ่วงของโลก ยังเกิดจากเกรเดียนท์ข องอุณภูมิในแนวระดับอีกด้วย ซึ่งเกรเดียนท์เหล่านี้ก่อให้เกิดแรงลอยตัวที่ทำให้เกิดการไหลของของ ใหลในวัสดุพรุน ส่งผลให้เกิดการถ่ายเทความร้อนโดยวิธีพาความร้อน รูปแบบการไหลเกิดเป็นคู่ ของ vortex ที่เรียงตัวในแนวระดับและหมุนในทิศทางดรงข้ามกัน นอกจากนั้นทิศการหมุนของ vortex ในกรณี ที่วัสดุพรุนได้รับความร้อนจะดรงข้ามกับกรณีที่วัสดุพรุนได้รับความเย็น สูตรการ คำนวณค่า Nusselt number ถูกพัฒนาขึ้นและนำมาช่วยในการวิเคราะห์พฤติกรรมการถ่ายเทความ ร้อนได้อย่างถูกด้อง จากการศึกษาพบว่า สัมประสิทธิ์การถ่ายเทความร้อน Rayleigh number, Darcy number หรือแม้แต่ทิศทางการเคลื่อนตัวของของไหลมีอิทธิพลต่อรูปแบบการไหลและการ ถ่ายเทความร้อน ในส่วนที่สอง เป็นการศึกษากระบวนการให้ความร้อนจากคลื่นไมโครเวฟโดยใช้ ท่อนำคลื่นทรงสี่เหลี่ยม แก่น้ำ และวัสดุพรุนซึ่งใช้ porous packed bed ซึ่งบรรจุด้วยลูกแก้ว และน้ำ จากผลการศึกษาพบว่าคุณสมบัติไดอิเล็คตริกของวัสดุพรุน ตำแหน่งการวางวัสดุ ขนาดของวัสดุ โดยเฉพาะอย่างยิ่ง ความหนา มีผลต่อกลไกลการถ่ายเทความร้อนในวัสดุ

Abstract

This research includes two main relevant parts. In the first part, the transient natural convection flow through a fluid-saturated porous medium in a square enclosure with a partial surface convection was investigated using Brinkmann-extended Darcy model. Physical problem consists of a rectangular cavity filled with porous medium. The cavity is insulated except the top wall that is partially exposed to an outside ambient. The formulation of differential equations is solved numerically under appropriate initial and boundary conditions using the finite difference method. The finite difference equations handling the convection boundary condition of the open top surface are derived. In addition to the negative density gradient in the direction of gravitation, a lateral temperature gradient in the region close to the top wall induces the buoyancy force under an unstable condition. The two-dimensional flow is characterized mainly by the clockwise and anti-clockwise symmetrical vortices driven by the effect of buoyancy. The directions of vortex rotation generated under the heating condition are in the opposite direction as compared to the cooling condition. Unsteady effects of associated parameters were examined. The modified Nusselt number (Nu) is systematically derived. This newly developed form of Nu captures the heat transfer behaviors reasonably accurately. It was found that the heat transfer coefficient, Rayleigh number, Darcy number as well as flow direction strongly influenced characteristics of flow and heat transfer mechanisms. In the second portion, the heating of liquid layer by microwave with rectangular wave guide has been investigated. Two different materials which are water and porous packed bed are examined. The porous bed is filled with uniform glass bead and water. In this work, effects of the dielectric properties, dimension and location of the heated material and microwave power level on the heating mechanism were examined. Based on a model combining the Maxwell and heat transport as well as fluid flow equations, the resulting solutions indicate that the heating kinetic strongly depends on the dielectric properties and geometry of material.

หน้าสรุปโครงการ (Executive Summary) ทุนพัฒนาศักยภาพในการทำงานวิจัยของอาจารย์รุ่นใหม่

·
1. ชื่อโครงการ
(ภาษาไทย) การวิเคราะห์พฤติกรรมการถ่ายเทความร้อนในช่องวัสดุพรุนที่ได้รับพลังงานความร้อน จากคลื่นไมโครเวฟโดยใช้ท่อนำคลื่นทรงสี่เหลี่ยม (เชิงทฤษฎีและการทดลอง)
(ภาษาอังกฤษ) Natural convection flow in cavity filled with porous material under the influence of microwave energy using a rectangular wave guide (theoretical and experimenta analysis)
2. ชื่อหัวหน้าโครงการ หน่วยงานที่สังกัด ที่อยู่ หมายเลขโทรศัพท์ โทรสาร และ e-mail
ภาควิชาวิศวกรรมเครื่องกล คณะวิศวกรรมศาสตร์ มหาวิทยาลัยธรรมศาสตร์ศูนย์
รังสิต ตำบล คลองหนึ่งอำเภอ คลอง หลวง
จังหวัดปทุมธานี
รหัสไปรษณีย์12120
โทรศัพท์02-5643001-9ต่อ 3143โทรสาร02-
e-mailpwatit@engr.tu.ac.th
3. สาขาวิชาที่ทำการวิจัยวิศวกรรมเครื่องกล
5. ระยะเวลาดำเนินงาน
6. ได้เสนอโครงการนี้ หรือโคร [์] งการที่มีส่วนเหมือนกับเรื่องนี้บางส่วนเพื่อขอทุนต่อแหล่งทุนอื่นที่ ใดบ้าง
[7] ໃນປີຄັດສາດຕ່ວມຂອງການວຶ່ນ

7. ปัญหาที่ทำการวิจัย และความสำคัญของปัญหา

การวิจัยที่ศึกษาเกี่ยวกับกรรมวิธีการให้ความร้อนโดยอาศัยพลังงานจากคลื่น ไมโครเวฟกำลังเป็นที่สนใจอย่างกว้างขวางขึ้นเป็นลำดับ เนื่องจากข้อได้เปรียบต่าง ๆทั้งในส่วนของ คุณภาพและเวลาที่ใช้ (Feng and Tang [1], Feng et al. [2] และ Ratanadecho et al. [3-4, 8-10]) เหนือกรรมวิธีให้ความร้อนแบบทั่วไป (conventional heating) หรือแม้แต่การใช้พลังงานจาก แสงอาทิตย์หรือพลังงานจากลมร้อน ซึ่งการให้ความร้อนด้วยวิธีเหล่านี้ใช้หลักการถ่ายเทความร้อนโดย อาศัยภวามแตกต่างของอุณหภูมิที่บริเวณผิวนอกกับผิวชั้นในของวัสดุหรือผลิตภัณฑ์ ด้วยการให้ความ ร้อนจากผิวนอก ถ่ายเทเข้าสู่ผิวชั้นใน แต่สำหรับหลักการถ่ายเทความร้อนของการให้ความร้อนโดยใช้ ไมโครเวฟ (microwave heating) จะเป็นลักษณะเชิงปริมาดรโดยคลื่นไมโครเวฟจะแผ่รังสีทั่วทั้งก้อน วัสดุในเวลาเดียวกันโดยอาศัยคุณสมบัติการดูดกลินพลังงานจากคลื่นไมโครเวฟของตัววัสดุนั้น ส่งผลให้เกิดการกระจายความร้อนเป็นอย่างสม่ำเสมอทั่วทั้งปริมาดร (volumetric heating)

ปัจจุบันการให้ความร้อนวิธีไมโครเวฟถูกนำมาใช้ในงานหลายด้าน เช่นการอบแห้ง (drying), การ อบยาง (vulcanization of rubber), และการฆ่าเชื้อโรคในอาหาร (sterilization) เป็น ต้น นอกจากนี้วัสดุทั่วไปในงานอุตสาหกรรมต่างๆไม่ว่าจะเป็นไม้, ยาง, อาหาร, ผลิตภัณฑ์ทาง การเกษตร และอื่นๆจัดเป็นวัสดุพรุน (porous material) ทั้งสิ้น กล่าวคือดัววัสดุประกอบด้วย 3 สถานะ ได้แก่ สถานะของแข็งหรือ matrix และของเหลวหรือก๊าช ที่อยู่ในช่องว่าง (void) การศึกษา ถึงกลไกการถ่ายเทความร้อนและมวลสารในวัสดุพรุนถือเป็นศาสตร์แขนงใหม่ที่มีความสำคัญอย่าง ยิ่ง ซึ่งศาสตร์แขนงนี้เป็นส่วนหนึ่งของงานวิจัยนี้ด้วย

ที่ผ่านมางานวิจัยในเรื่องการถ่ายเทความร้อนในวัสดุพรุนยังจำกัดอยู่กับการให้ความ ร้อนจากแหล่งกำเนิดแบบธรรมดาที่กล่าวไว้แล้วข้างต้น โดยเฉพาะการศึกษาการกระจายตัวของ อุณหภูมิ (temperature distribution) และการกระจายตัวของความเร็ว (velocity distribution) ในช่อง สี่เหลี่ยมที่บรรจุด้วยวัสดุพรุนอิ่มตัวด้วยน้ำ (cavity flow in saturated porous media) (Khanafer and Chamkha [5], Al-Amiri [6], และ Khanafer and Vafai [7]) ยังมีการศึกษากันน้อย โดยเฉพาะ อย่างยิ่งการให้ความร้อนแบบบางส่วนซึ่งเป็นส่วนของงานวิจัยนี้ ที่ผ่านมามีการศึกษาน้อยมาก (Oztop, [11]) รายละเอียดของงานวิจัยที่ผ่านมาอยู่ในส่วนเนื้อหา.

ในส่วนของการศึกษาการทำความร้อนด้วยพลังงานจากคลื่นไมโครเวฟก็ยังมีการศึกษา กันน้อยมาก Ratanadecho et al. [8] นำเสนอรางานวิจัยที่ถือเป็นงานวิจัยชิ้นแรกที่มีความสมบูณ์ทั้ง เชิงทฤษฎีและการทดลองของการทำความร้อนด้วยพลังงานจากคลื่นไมโครเวฟ อย่างไรก็ตาม งานวิจัยนี้พิจารณาให้ชิ้นทดสอบเป็นชั้นของของเหลวเท่านั้น ไม่ได้พิจารณาเป็นวัสดุพรุน สำหรับ งานวิจัยที่เกี่ยวข้องกับการให้ความร้อนจากคลื่นไมโครเวฟในชิ้นทดสอบที่เป็นวัสดุพรุนที่บรรจุด้วย ของเหลวนั้นยังไม่มีการทำมาก่อน เนื่องมาจากความซับซ้อนของปรากฏการณ์ที่เกี่ยวข้องกับสถานะ ของสสารหลายชนิด คุณสมบัติด้านความร้อนประสิทธิผล (effective thermal property) คุณสมบัติ ด้านชลศาสตร์ (hydrodynamic property) ตลอดจนคุณลักษณะการเคลื่อนด้วของของเหลวในวัสดุ พรุน

ดังนั้นในงานวิจัยที่กำลังเสนอนี้จะศึกษาการถ่ายเทความร้อนในวัสดุพรุนที่ได้รับความร้อนทั้งแบบบางส่วนด้วยวิธีพาความร้อนและแบบที่ได้รับพลังงานจากคลื่นไมโครเวฟ งานวิจัยนี้ มุ่งเน้นการศึกษาโดยอาศัยพื้นฐานทางทฤษฎีในโครงสร้างระคับจุลภาค (microscopic level) เพื่อ พัฒนาแบบจำลองทางคณิตศาสตร์ของการถ่ายเทความร้อนเพื่อทำนายและศึกษาพฤติกรรมการถ่ายเทความร้อน, การเปลี่ยนแปลงพารามิเตอร์ที่เกี่ยวข้อง, การกระจายตัวของอุณหภูมิ และลักษณะการเคลื่อน ตัวของของไหลในช่องว่างของรูพรุนอันเนื่องมาจากความร้อนที่เกิดขึ้นภายซึ่งเกิดจากจากพลังงานคลื่น ไมโครเวฟ ผลงานวิจัยนี้จะเป็นผลงานชิ้นแรกในระคับนานาชาติที่ได้ศึกษาถึงรูปแบบการไหลของ ของเหลวในวัสดุพรุนและลักษณะการกระจายตัวของความร้อนในชิ้นทคสอบที่ได้รับคลื่นไมโครเวฟ กวามถี่ 2.45 GHz ที่โหมด TE_{เอ}ในท่อนำคลื่นทรงสี่เหลี่ยม องค์ความรู้ที่ได้รับจากงานวิจัยขึ้นนี้จะมี ประโยชน์อย่างสูงต่ออุตสาหกรรมอาหาร หรืออุตสาหกรรมแปรรูปผลผลิตทางการเกษตรที่เนื้อวัสดุมี ลักษณะเป็นวัสดุพรุน รวมไปถึงเทคโนโลยีการการเก็บรักษาเนื้อเยื่อในงานด้านการแพทย์ นอกจากนี้องค์ความรู้ดังกล่าวยังสามารถนำไปใช้วิเคราะห์เชิงลึกสำหรับปัญหาที่มีการเปลี่ยนสถานะ ของสสาร อาทิเช่น ปัญหาการเย็นเยือกในวัสดุพรุน (freezing in porous media) และปัญหาการทำ ละลายในวัสดุพรุน (melting in porous media) เป็นตัน

8. วัตถุประสงค์

เพื่อศึกษาพฤติกรรมการถ่ายเทความร้อน, การเปลี่ยนแปลงอุณหภูมิ, ความดันและ สนามความเร็ว (velocity field) ของการไหลในวัสดุพรุนภายใต้อิทธิพลของพลังงานจากคลื่น ไมโครเวฟโดยอาศัยแบบจำลองทางคณิตศาสตร์ที่จะถูกพัฒนาขึ้นในงานวิจัยนี้ประกอบกับผลจาก การทดลอง ผลการศึกษาก่อให้เกิดความเข้าใจถึงองค์ความรู้พื้นฐานในกระบวนการถ่ายเทความร้อน ในวัสดุพรุนและผลกระทบจากคลื่นไมโครเวฟ ทำให้สามารถใช้พัฒนาการให้ความร้อนวิธีไมโครเวฟ พัฒนาการออกแบบสร้างอุปกรณ์ทดลองจริงในทางปฏิบัติให้มีประสิทธิภาพสูง และจะสามารถนำไป ประยุกต์ใช้และพัฒนาระบบการให้ความร้อนในงานอุตสาหกรรมต่างๆที่เกี่ยวข้องต่อไป

9. ระเบียบวิธีวิจัย

พัฒนาแบบจำลองทางคณิตศาสตร์อาศัยข้อมูลจากการคันก็ว้างานวิจัยที่เกี่ยวข้องและ พื้นฐานทางทฤษฎี โดยใช้ระเบียบวิธีการคำนวณเชิงตัวเลขชั้นสูงอาศัยเทคนิค FVM (Finite Element Method) และ FDTD (Finite Difference Time Domain) เพื่อหาคำตอบของปัญหาการ ถ่ายเทความร้อนในวัสดุพรุนทั้งกรณีที่ได้รับความร้อนแบบทั่วไปและกรณีที่ได้รับความร้อนจาก พลังงานไมโครเวฟ ซึ่งสามารถอธิบายได้จากกลุ่มของสมการอนุพันธ์ที่ไม่เป็นอิสระต่อกัน (coupled) และมีความไม่เชิงเส้นสูง (highly non-linear) อันประกอบไปด้วยสมการอนุพันธ์ย่อยมวล โมเมนดัม และพลังงาน ชุดสมการอนุพันธ์ย่อย Darcy และสมการ Maxwell (3 มิติ) และข้อมูลบางส่วนที่ได้ สามารถนำมาเปรียบเทียบกับผลจากการทดลองที่ใช้เครื่องควบคุมระบบการให้ความร้อนจาก พลังงานไมโครเวฟแบบมีช่องน้ำคลื่นความถี่ 2.45 GHz ที่โหมด TE₁₀ จากนั้นผลโดยรวมทั้งหมดจะ ถูกนำมาวิเคราะห์และสรุป

เอกสารอ้างอิง

- 1. Feng, H., and Tang, J., 1998, "Microwave Finish Drying of Diced Apples in a Spouted Bed," J. Food. Sci., 63, No. 4, pp. 679-683.
- Feng, H., Tang, J., and Cavalien, R. P., 1999, "Combined Microwave and Spouted Bed Drying of Diced Apples: Effect of Drying Conditions on Drying Kinetics and Product Temperature," Drying Technol., 17, No. 10, pp. 1981-1998.
- Ratanadecho, P., Aoki, K. and Akahori, M., "Influence of Irradiation Time, Particle Sizes and Initial Moisture Content During Microwave Drying of Multi-Layered Capillary Porous Materials," ASME J. Heat Transfer, Vol. 124 (1), 2002, pp. 151-161.
- Ratanadecho, P., Aoki, K. and Akahori, M., "Experimental Validation of a Combined Electromanetic and Thermal Model for a Microwave Heating of Multi-Layered Materials Using a Rectangular Wave Guide," ASME J. Heat Transfer, Vol. 124(5), 2002, pp. 992-996.
- Khanafer, K. M. and Chamkha, A. J., "Mixed convection flow in a lid-driven enclose filled with a fluid-saturated porous medium," Int. J. Heat Mass Transfer, Vol. 42, 1999, pp. 2465-2481.
- Amiri, A. M., "Analysis of momentum and energy transfer in a lid-driven cavity filled with a porous medium," Int. J. Heat and Mass Transfer, Vol. 43, 2000, pp. 2465-2481.
- Khanafer, K. M. and Vafai, K, "Double-diffusive mixed convection in a lid-driven enclosure filled with saturated porous medium," Numerical Heat Transfer, Vol. 42, 2002, pp. 465-486.
- Ratanadecho, P., Aoki, K. and Akahori, M., " A Numerical and Experimental Investigation of the Modeling of Microwave Heating for Liquid Using a Rectangular Wave Guide (Effect of Natural Convection and Electrical Conductivity)," Appl. Math. Modelling, Vol. 26(3), 2002, pp. 449-472.
- Ratanadecho, P., Aoki, K. and Akahori, M., "A numerical and experimental investigation of microwave drying using a rectangular wave guide," Drying Technol. J., Vol. 19 (9), 2001, pp 2209-2234.

- 10. Ratanadecho, P., Aoki, K. and Akahori, M., " A numerical and experimental investigation of the modeling of microwave melting of frozen packed beds using a rectangular wave guide," Int. Comm. Heat Mass Transfer, Vol. 28, 2001, pp. 751-762.
- 11. Oztop, H.F., "Natural convection in partially cooled and inclined porous rectangular enclosure," International Journal of Thermal Sciences, Vol. 46, 2007, pp. 149-156.

เนื้อหางานวิจัย

1. ส่วนประกอบของงานวิจัย

งานวิจัยนี้แบ่งออกได้เป็น 2 ส่วนหลักคือ

- 1.1 การวิเคราะห์การพาความร้อนแบบธรรมชาติในช่องวัสดุพรุนที่ได้รับความร้อนบางส่วน (Analysis of Natural Convection in Porous Cavity with Partial Convection Boundary Condition)
- 1.2 การวิเคราะห์กระบวนการให้ความร้อนด้วยคลื่นไมโครเวฟแก่วัสดุพรุนไดอิเล็คตริค (Analysis of Microwave Heating of Dielectric Materials Using a Rectangular Wave Guide)

งานวิจัยทั้ง 2 ส่วนนี้มีความเกี่ยวข้องกัน ส่วนแรกศึกษาการถ่ายเทความร้อนแบบบางส่วนแก่ วัสดุพรุนโดยมีการให้ความร้อนแบบพาความร้อนแบบธรรมชาติ ไม่อาศัยพลังงานจากคลื่น ไมโครเวฟ ในงานวิจัยอีกส่วนหนึ่ง นอกจากการให้ความร้อนโดยวิธีพาความร้อนแล้ว มีการให้ ความร้อนจากคลื่นไมโครเวฟอีกด้วย รายละเอียดการวิจัยทั้ง 2 ส่วนแสดงไว้ในหัวข้อถัดไป

2. รายละเฮียดของเนื้อหา

ส่วนที่ 1

2.1 Analysis of Natural Convection in Porous Cavity with Partial Convection Boundary

Condition

1. Introduction

The convective heating or cooling that causes heat and fluid flows inside cavity is found in various applications including lakes and geothermal reservoirs, underground water flow, solar collector etc. (Bergman et al., 1986). Associated industrial applications include secondary and tertiary oil recovery, growth of crystals (Imberger and Hamblin, 1982), heating and drying process (Stanish et al., 1986; Rattanadecho et al., 2001, 2002), solidification of casting, sterilization etc. Natural or free convection in a porous medium has been studied extensively. Cheng (1978) provides a comprehensive review of the literature on free convection in fluid-saturated porous media with a focus on geothermal systems. In the framework of porous media models, Darcy proposed the phenomenological relation between the pressure drop across a saturated porous medium

and the flow rate. The Darcy model has been employed in the recent investigations. Bradean et al. (1997) assumed Darcy's law and used Boussinesq approximation to numerically simulate the free convection flow in a porous media adjacent to vertical or horizontal flat surface. The surface is suddenly heated and cooled sinusoidally along its length. The Darcy law with the Boussinesq approximation was also employed by Bilgen and Mbaye (2001) to study the development of Be'n-ard cell in fluid-saturated porous cavity whose lateral walls are cooled. It was found that two convective solution branches exist that are related to the Darcy-Rayleigh and Biot numbers. Recently, a numerical study was conducted to solve the problem of thermosolutal convection within a rectangular enclosure (Bera and Khalili, 2002). The results revealed that anisotropy causes significant changes in Nusselt and Sherwood numbers. Many works of flow in porous media, such as ones addressed above, have used the Darcy law. Although the Darcy law is applicable to slow flows, it does not account for initial and boundary effects. In the situation when the flow is strong, and solid boundary effect and viscous effect are not negligible, these effects termed non-Darcy effects, become important (Khanafer and Chamkha, 1998). Bera et al. (2002) considered double diffusive convection due to constant heating and cooling on the two vertical walls, based on a non-Darcy model inclined permeability tensor. Two distinguished modifications of Darcy' law are the Brinkmann's and the Forchheimer's extensions which treats the viscous stresses at the bounding walls and the non-linear drag effect due to the solid matrix respectively (Nithiarasu et al., 1997). The Brinkman-extended Darcy model has been considered in a literature (Tong and Subramanian, 1985; Laurat and Prasad, 1987). Darcy-Forchheimer model has been used in a number of published works (Beckermann et al., 1985; Lauriat and Prasad, 1989; Basak, 2006). In the study of effects of various thermal boundary conditions applied to saturated porous cavity, the conduction dominant regime is within $Da \le 10^{-5}$. Nithiarasu et al. (1998) examined effects of applied heat transfer coefficient on the cold wall of the cavity upon flow and heat transfer inside a porous medium. The differences between the Darcy and non-Darcy flow regime are clearly investigated for different Darcy, Rayleigh and Biot numbers and aspect ratio. Variations in Darcy, Rayleigh and Biot numbers and aspect ratio significantly affect natural flow convective pattern.

Natural convection flows with a variety of configurations were investigated for different aspects. Oosthuizen and Patrick (1995) performed numerical studies of natural

convection in an inclined square enclosure with part of one wall heated to a uniform temperature and with the opposite wall uniformly cooled to a lower temperature and with the remaining wall portions. The enclosure is partially filled with a fluid and partly filled with a porous medium, which is saturated with the same fluid. The main results considered were the mean heat transfer rate across the enclosure. Nithiarasu et al. (1997) examined effects of variable porosity on convective flow patterns inside a porous cavity. The flow is triggered by sustaining a temperature gradient between isothermal lateral walls. The variation in porosity significantly affects natural flow convective pattern. Khanafer and Chamkha (1998) performed numerical study of mixed convection flow in a lid-driven cavity filled with a fluid-saturated porous media. In this study, the influences of the Richardson number, Darcy number and the Rayleigh number play an important role on mixed convection flow inside a square cavity filled with a fluid-saturated porous media. Recently, Al-Amiri (2000) performed numerical studies of momentum and energy transfer in a lid-driven cavity filled with a saturated porous medium. In this study, the force convection is induced by sliding the top constant-temperature wall. It was found that the increase in Darcy number induces flow activities causing an increase in the fraction of energy transport by means of convection. With similar description of the domain configuration, Khanafer and Vafai (2002) extended the investigation to mass transport in the medium. The buoyancy effects that create the flow are induced by both temperature and concentration gradients. It was concluded that the influences of the Darcy number, Lewis number and buoyancy ratio on thermal and flow behaviors were significant. Furthermore, the state of art regarding porous medium models has been summarized in the recently published books (Basak et al., 2006; Nield and Bejan, 1999; Vafai, 2000; Pop and Ingham, 2001).

Previous investigations have merely focused on momentum and energy transfer in cavity filled with a saturated porous medium subjected to prescribed temperature and prescribed wall heat flux conditions. However, only a very limited amount of numerical and experimental work on momentum and energy transfer in a cavity filled with a saturated porous medium subjected to heat transfer coefficient boundary condition at the exposed portion of the top wall has been reported. Moreover, only very few published work is pertinent to partially heated or cooled porous media although they are found in a number of applications such as in flush mounted electrical heater or buildings (Al-Amiri, 2002; Oztop, 2007). The very recent work of Oztop (2007) investigated natural

convection in partially cooled and inclined porous enclosures. His study presented the steady state results within the enclosure of isothermal heated and cooled walls. In our study, the surface is partially cooled under the convective boundary condition, allowing the surface temperature to change with time. The convective cooling condition or so-called condition of the third kind is systematically derived. While the focus of the present study is on the cooling effect, our recently published work (Pakdee and Rattanadecho, 2006) with similar schematic of the domain studied the influence of partially heated surface on thermal/flow behaviors. The results were qualitatively discussed in detail. However, no quantitative description of heat transfer in terms of Nusselt number (Nu) was reported. To the best knowledge of the authors, no attention has been paid to transient convection due to surface partial convection.

In the present study, the quantitative study in terms of Nu is taken into account. The new formulation of Nu is developed to correctly capture heat transfer behaviors. The study of heat transfer due to cooling condition has been carried out for transient natural convective flow in a fluid-saturated porous medium filled in a square cavity. In contrast to the heating condition, the cooling condition changes the direction of the induced flows. The top surface is partially open to the ambient, allowing the surface temperature to vary, depending on the influence of convection heat transfer mechanism. Computed results are depicted using temperature, flow distributions and heat transfer rates in terms of local and average Nusselt numbers. The influences of associated parameters such as heat transfer coefficient, Rayleigh number and Darcy number on the flow and thermal configurations were examined.

2. Problem Description

The computational domain, depicted in figure. I is a rectangular cavity of size W×H filled with a fluid-saturated porous medium. Aspect ratio of unity (A=1) is used in the present study. The domain boundary is insulated except the top wall, which is partially exposed to an ambient air. The initial and boundary conditions corresponding to the problem are of the following forms.

$$u = v = 0$$
, $T = T_i$ for $t = 0$ (1)

$$u = v = 0 \quad \text{at } x = 0, W \qquad 0 \le y \le H$$

$$u = v = 0 \quad \text{at } y = 0, H \qquad 0 \le x \le W$$
(2)

$$\frac{\partial T}{\partial x} = 0 \quad \text{at } x = 0, W \qquad 0 \le y \le H$$

$$\frac{\partial T}{\partial y} = 0 \quad \text{at } y = 0 \qquad 0 \le x \le W$$

$$\frac{\partial T}{\partial y} = 0 \quad \text{at } y = H \quad 0 \le x \le L \text{ and } W-L \le x \le W$$
(3)

The boundary condition at the exposed portion of the top wall is defined as

$$-k\frac{\partial T}{\partial y} = h[T_{\infty} - T] \quad \text{at } y = H \qquad L \le x \le W-L, \tag{4}$$

where k and h are effective thermal conductivity and convection heat transfer coefficient. Symbols ϵ and ν denotes porosity of porous medium and fluid viscosity, respectively. This type of condition corresponds to the existence of convective heat transfer at the surface and is obtained from the surface energy balance.

The porous medium is assumed to be homogeneous and thermally isotropic. The saturated fluid within the medium is in a local thermodynamic equilibrium with the solid matrix (El-Refaee et al., 1998; Al-Amiri, 2002). The porous porosity is uniform. The fluid flow is unsteady, laminar and incompressible. The pressure work and viscous dissipation are all assumed negligible. The thermophysical properties of the porous medium are taken to be constant. However, the Boussinesq approximation takes into account of the effect of density variation on the buoyancy force. Furthermore, the solid matrix is made of spherical particles, while the porosity and permeability of the medium are assumed to be uniform throughout the rectangular cavity. Using standard symbols, the governing equations describing the heat transfer phenomenon are given by

$$\frac{\partial u}{\partial x} + \frac{\partial v}{\partial y} = 0$$

$$\frac{1}{\varepsilon} \frac{\partial u}{\partial t} + \frac{u}{\varepsilon^2} \frac{\partial u}{\partial x} + \frac{v}{\varepsilon^2} \frac{\partial u}{\partial y} = -\frac{1}{\rho_f} \frac{\partial P}{\partial x} + \frac{v}{\varepsilon} \left(\frac{\partial^2 u}{\partial x^2} + \frac{\partial^2 u}{\partial y^2} \right)$$

$$-\frac{\mu u}{\rho_f \kappa}$$

$$\frac{1}{\varepsilon} \frac{\partial v}{\partial t} + \frac{u}{\varepsilon^2} \frac{\partial v}{\partial x} + \frac{v}{\varepsilon^2} \frac{\partial v}{\partial y} = -\frac{1}{\rho_f} \frac{\partial P}{\partial y} + \frac{v}{\varepsilon} \left(\frac{\partial^2 v}{\partial x^2} + \frac{\partial^2 v}{\partial y^2} \right)$$
(6)

$$\frac{1}{\varepsilon} \frac{\partial}{\partial t} + \frac{1}{\varepsilon^2} \frac{\partial}{\partial x} + \frac{1}{\varepsilon^2} \frac{\partial}{\partial y} = -\frac{1}{\rho_f} \frac{\partial}{\partial y} + \frac{1}{\varepsilon} \left(\frac{\partial}{\partial x^2} + \frac{\partial}{\partial y^2} \right) + g \beta (T - T_{\infty}) - \frac{\mu v}{\rho_c \kappa}$$

$$ho_f \kappa$$
 $\partial T = \partial T = \left(\partial^2 T + \partial^2 T\right)$

(7)

$$\sigma \frac{\partial T}{\partial t} + u \frac{\partial T}{\partial x} + v \frac{\partial T}{\partial y} = \alpha \left(\frac{\partial^2 T}{\partial x^2} + \frac{\partial^2 T}{\partial y^2} \right)$$
(8)

$$\sigma = \frac{\left[\varepsilon(\rho c_p)_f + (1-\varepsilon)(\rho c_p)_s\right]}{(\rho c_p)_f},\tag{9}$$

where κ is medium permeability, β is thermal expansion coefficient, α is effective thermal diffusivity of the porous medium, μ and ν are viscosity and kinematic viscosity of the fluid respectively. In the present study, the heat capacity ratio σ is taken to be unity since the thermal properties of the solid matrix and the fluid are assumed identical (Bergman et al., 1986; Khanafer and Vafai, 2002). The momentum equation consists of the Brinkmann term, which describes viscous effects due to the presence of solid body (Brinkmann, 1947). This form of momentum equation is known as Brinkmann-extended Darcy model. Lauriat and Prasad (1987) employed the Brinkmann-extended Darcy formulation to investigate the buoyancy effects on natural convection in a vertical enclosure. Although the viscous boundary layer in the porous medium is very thin for most engineering applications, inclusion of this term is essential for heat transfer calculations (Al-Amiri, 2000). However, the inertial effect was neglected, as the flow was relatively low.

The variables are transformed into the dimensionless quantities defined as,

$$X = \frac{x}{H}, Y = \frac{y}{H}, \tau = \frac{t\alpha}{H^{2}}, U = \frac{uH}{\alpha}, V = \frac{vH}{\alpha}$$

$$\zeta = \frac{\omega H^{2}}{\alpha}, \Psi = \frac{\psi}{\alpha}, \theta = \frac{T - T_{I}}{T_{L} - T_{I}}$$
(10)

where ω and ψ represent dimensional vorticity and stream function, respectively. Symbol α denotes thermal diffusivity. Temperatures T_l and T_h change their values according to the problem type. In the heating case, T_l is initial temperature of a medium, and T_h is an

ambient temperature. In the other case of cooling, T_h is set to be an initial temperature of the medium, while T_l is an ambient temperature instead. Thus the dimensionless form of the governing equations can be written as

$$\frac{\partial^{2} \psi}{\partial X^{2}} + \frac{\partial^{2} \psi}{\partial Y^{2}} = -\varsigma$$

$$\varepsilon \frac{\partial \zeta}{\partial \tau} + U \frac{\partial \zeta}{\partial X} + V \frac{\partial \zeta}{\partial Y} = \varepsilon \Pr\left(\frac{\partial^{2} \zeta}{\partial X^{2}} + \frac{\partial^{2} \zeta}{\partial Y^{2}}\right) + \varepsilon^{2} \operatorname{Ra} \Pr\left(\frac{\partial \theta}{\partial X}\right) - \frac{\varepsilon^{2} \operatorname{Pr}}{\operatorname{Da}} \varsigma \quad (12)$$

$$\sigma \frac{\partial \theta}{\partial \tau} + U \frac{\partial \theta}{\partial X} + V \frac{\partial \theta}{\partial Y} = \alpha \left(\frac{\partial^{2} \theta}{\partial X^{2}} + \frac{\partial^{2} \theta}{\partial Y^{2}}\right), \quad (13)$$

where the Darcy number, Da is defined as κ/H^2 , and $Pr = \nu/\alpha$ is Prandtl number, where $\alpha = k_e/(\rho c_p)_f$ is the thermal diffusivity. The Rayleigh number Ra, which gives the relative magnitude of buoyancy and viscous forces, is defined as $Ra = g \beta (T_i - T_m) H^3/(\nu \alpha)$.

3. Numerical Procedure

The thermal properties of the porous medium are taken to be constant. Specific heat ratio of unity is assumed. The effective thermal conductivity of the porous medium considered is 10 W/m·K.

In the present study, the iterative finite difference method is used to solve the transient dimensionless governing equations (Eqs. (10)-(12)) subject to their corresponding initial and boundary conditions given by Eqs. (1)-(4). Approximation of convective terms is based on an upwind finite differencing scheme, which correctly represent the directional influence of a disturbance. A uniform grid resolution of 61 × 61 was found to be sufficient for all smooth computations and computational time required in achieving steady-state conditions. Finer grids did not provide a noticeable change in the computed results.

3.1 Convection boundary condition

The finite difference form of boundary condition at the open part of the top surface is systematically derived, based on energy conservation principle. The boundary values of dimensionless temperature of a node i, j $\theta_{i,j}$ in the heating case are expressed as

$$\theta_{ij} = \frac{2\theta_{ij-1} + \theta_{i-1j} + \theta_{i+1j} + 2\frac{h\Delta y}{k}}{2(\frac{h}{k}\Delta Y + 2)},$$
(14)

where ΔY is the mesh size in y-direction.

In the different case of cooling phenomenon, the expression is given by

$$\theta_{ij} = \frac{2\theta_{ij-1} + \theta_{i-1j} + \theta_{i+1j}}{2(\frac{h}{k}\Delta Y + 2)}$$
(15)

It can be noticed that both the equations (14) and (15) are independent of an ambient temperature T_{∞} as it has been eliminated during the derivation. This feature is attractive since the solutions can be obtained regardless of a value of T_{∞} .

3.1 Corrected formulation of Nusselt number

The local Nusselt number (Nu) at the cooled horizontal surface is used as a tool to determine the ratio of convection heat transfer to conduction heat transfer within the porous enclosure. The accurate derivation of Nu is extremely important from the standpoint of determining the rate of heat transfer occurring at a surface. Based on the concept of energy balance at the surface,

$$-k\frac{dT}{dy}\bigg|_{y=H} = h(T_H - T_{\infty}), \qquad (16)$$

where H is indicated in figure 1, and with the definition of Nu,

$$Nu = \frac{hH}{k} = -\frac{H}{(T_H - T_{\infty})} \frac{dT}{dy} \bigg|_{Y=H}$$
 (17)

In terms of the dimensionless quantities θ and Y defined in the preceding equation (10), Nu will take the form,

$$Nu = -\frac{1}{\theta_H} \frac{d\theta}{dy} \bigg|_{Y=1}, \qquad (18)$$

where θ_H is the dimensionless temperature at the top surface.

The new formulation of Nu in the present work has not yet been found in the literature. This modified form of Nu takes into account of temperature variation at the cooled surface. The average Nusselt Number, Nu is computed according to

$$\overline{\text{Nu}} = \int_{L}^{W-L} \frac{\text{Nu}(x)dx}{I}, \qquad (49)$$

where l is the length of the gap at the top wall.

In order to verify the accuracy of the present numerical study, the results obtained by the present numerical model were validated against the results obtained by Aydin (2000) for a free convection flow in a cavity, with side-heated isothermal wall, filled with pure air (Pr = 0.7) for Rayleigh number of 10^4 . It was found that the solutions have good agreement with the previously published work. The results of the selected test case are illustrated in figures. 2 for streamlines and temperature contour lines. The results of selected tests are given in table 1 that shows a good agreement of the maximum value of the stream function and the maximum values of the horizontal and vertical velocity components between the present solution and that of Aydin. Also, the results from the present numerical model were compared with the solution of Nithiarasu et al. (1997) in the presence of porous medium for additional source of confidence, as shown in figures.

3. The values of $Ra = 10^4$, Da = 0.01 and $\varepsilon = 0.6$ were chosen. Table 2 clearly shows a good agreement of the maximum values of the stream function and vertical velocity component between the present solution and that of Nithiarasu et al (1997). All of these favorable comparisons lend confidence in the accuracy of the present numerical model.

4. Results and Discussion

The following discussions include the numerical results from the present study. Initial values of θ for an entire domain are set 0, based on equation (10) since the ambient temperature is higher than temperature of the medium in cavity. The investigations were conducted for a range of controlling parameters, which are Darcy number (Da) Rayleigh number (Ra) and convective heat transfer coefficient (h). The porosity ϵ of 0.8 and unity aspect ratio (A=1) were considered throughout in the present study. In order to assess global effects of these parameters, the streamlines and isotherm distributions inside the entire cavity are presented. All the figures have the same range of contour levels to

facilitate direct comparisons. The resulting computational fields were extracted at the time adequately long to ensure sufficient energy transferred throughout the domain. Figure 3 displays instantaneous images of the contour plots during the thermal and flow evolution. The Darcy number of 0.01, Pr = 1.0, $h = 60 \text{ w/m}^2\text{K}$, and $\varepsilon = 0.8$ are considered. The two columns represent temperature and stream function. With the same contour levels, comparisons can be observed directly. The four snapshots from top to bottom in each column are results taken at the dimensionless times $\tau = 0.0125, 0.09, 0.1675, \text{ and } 0.2475$ with the time interval. The vertical temperature stratification is observed. The streamline contours exhibit circulation patterns, which are characterized by the two symmetrical vortices. The fluid flows as it is driven by the effect of buoyancy. This effect is distributed from the top wall of cavity where the fluid is heated through the partially open area. This indicates the non-uniform temperature at the top surface, leading to an unstable condition. Thus the buoyancy effect is associated with the lateral temperature gradient at locations near the top surface. Heated portions of the fluid become lighter than the rest of fluid, and are expanded laterally away from the center to the sides then flow down along the two vertical walls, leading to the clockwise and counter-clockwise flow circulations. These results suggest that the buoyancy forces are able to overcome the retarding influence of viscous forces. An increase in strength of the vortices develops fast during early simulation times, and its maximum magnitude reaches 0.1 at $\tau = 0.0475$. After this time, the vortices are slowly weakened. Similarly, temperature distribution progressively evolves relatively fast in the early times. After the time $\tau = 0.07$, slow evolution is observed. This result corresponds to the decrease in strength of flow circulations. In the remaining area, the fluid is nearly stagnant suggesting that conduction is dominant due to minimal flow activities. This is because the viscous effects are large.

Figures 4 illustrates how the convective heat transfer coefficient influences thermal and flow behaviors, while other parameters Da = 0.1, Pr = 1.0, and $\varepsilon = 0.8$ are fixed. The variable values of h chosen are 60 and 300 W/m²·K, which may represent a typical free and forced convection, respectively. In all the figures henceforth, directions and magnitudes of the arrows indicate the direction as well as strength of the flows respectively. It is seen on the left column in figure 4 that the temperature gradients are steep at the top area near the exposed convective surface and gradually decreases toward the bottom of the domain. In the remaining area of the cavity, the temperature gradients are small and this implies that the temperature differences are very small in the bottom

region of the cavity where viscous effects are strong. It can be observed on the right-column plots, which presents streamline contours that the chance in h does not contribute a significant modification to the temperature contours. However, an increase in h expands temperature distribution area due to the more energy that is carried away from the location of convection surface condition toward the bottom. Moreover, higher value of h increases maximum temperature resulting in wider temperature range in the domain.

Effects of the Darcy number on the fluid flow and temperature inside the rectangular cavity are depicted in figure 5. The contour of isotherms and streamlines are plotted for different Darcy numbers while ε , Pr and h are kept at 0.8, 1.0 and 60 w/m²K respectively. The Darcy number, which is directly proportional to the permeability of the porous medium, was set to 0.001 and 0.1. The case in which the porous medium is absent corresponds to infinite Darcy number. The presence of a porous medium within rectangular enclosure results in a force opposite to the flow direction which tends to resist the flow which corresponds to suppress in the thermal currents of the flow as compared to a medium with no porous (infinite Darcy number). It is evident that the increase in Da enhances the streamline intensities thereby assisting downward flow penetration, which causes the streamline lines, i.e., two symmetrical vortices to stretch further away from the top surface. This results in expanding the region for which the convection significantly influences an overall heat transfer process. On the other hand, as the Darcy number decreases, the flow circulations as well as thermal penetration are progressively inhibited due to the reduced permeability of the medium except at the region close to the location of convection surface condition where the flow motions are relatively strong. Furthermore, figure 5c indicates that as Darcy number approaches zero, the convective heat transfer mechanism is almost suppressed, while the heat transfer by means of conduction plays an important role in heat transfer. The left column of figure 5 shows comparison of temperature in which the contours of different Darcy numbers appear roughly similar.

To gain further insight into the effects of the Darcy number on the thermally stratified layer, temperature contours for pure fluid are overlaid with that for porous fluid with Da of 0.001. The results are given in figure 6. It is noticed that temperature stratification layers, near the vertical symmetry line in the case of Da 0.001, move further downward relative to those for pure fluid. This observed incident results from a stronger flow in the upward direction in the central region for the pure medium. The upward flows inhibit the

thermal propagation. In contrast, in the areas away from the vertical center line, the downward flows assist heat to be transferred towards the bottom of the enclosure.

Figure 7 shows the isotherms and streamlines obtained for various Rayleigh numbers $(Ra = 10^3, 10^4 \text{ and } 10^5)$ whereas the Darcy number of 0.1, porosity of 0.8, and h of 60 w/m²K are fixed. The Rayleigh number provides the ratio of buoyancy forces to change in viscous forces. As Rayleigh number increases, the buoyancy-driven circulations inside the enclosure become stronger as seen from greater magnitudes of stream function. For the large value of Ra $(Ra = 10^5)$, there appears a pair of secondary weak circulations in the bottom region of the enclosure. The two vigorous vortices are confined to the upper domain, where convection is a dominant mode of heat transfer.

Although the profiles of temperature contour are qualitative similar, figure 8 displays overlaid contours for the two cases which are of $Ra = 10^3$ and $Ra = 10^5$. It is evident in the case of $Ra = 10^3$ that temperature contour lines penetrates faster relative to the low Ra case at the central locations around vertical symmetric line, but they move slower in the regions near the vertical walls. The results are consistent with the thermal behaviors observed in figure 6 for the same reasoning, which confirm how a flow direction impacts the convection heat transfer. Therefore it can be concluded to an interesting note that not only an intensity of a flow, but also the direction of the fluid flow locally affects the heat convection process.

In what follow, the numerical results for the cooling scenario are discussed. Initial values of θ for an entire domain are set to 1, based on equation (10) as the ambient temperature is lower than temperature of the medium in cavity. The investigations were conducted for a range of controlling parameters, which are Darcy number (Da) Rayleigh number (Ra) and convective heat transfer coefficient (h). The uniform porosity ϵ of 0.8 and unity aspect ratio (A=1) were considered throughout iff the present study. In order to assess global effects of these parameters, the streamlines and isotherm distributions inside the entire cavity are presented. All the figures have the same range of contour levels to facilitate direct comparisons.

The resulting computational fields were extracted at the time adequately long to ensure sufficient energy transferred throughout the domain. Figure 9 displays instantaneous images of the contour plots during the thermal and flow evolution. The Rayleigh number of $5x10^4$, Da = 0.1, Pr = 1.0, h = 60 w/m²K, and ε =0.8 are considered. The two columns represent contours of temperature and stream function respectively from

left to right. With the same contour levels, comparisons can be made directly. The four snapshots from top to bottom in each column are results taken at the dimensionless times $\tau = 0.013, 0.088, 0.168,$ and 0.245. The vertical temperature stratification is observed. The streamline contours exhibit circulation patterns, which are characterized by the two symmetrical vortices. The fluid flows as it is driven by the effect of buoyancy. This effect is distributed from the top wall of cavity where the fluid is cooled through the partially open surface, causing lower temperature near the top boundary. The existence of the nonuniform temperature along the top surface, and a decrease of density in the direction of gravitational force lead to an unstable condition. Thus the buoyancy effect is associated with the lateral temperature gradients at locations near the top surface. High temperature portions of fluid become lighter than the lower temperature portions at the middle where the wall is open. Theses light portions from two sides then expand laterally towards the center, compressing the lower temperature portions, which are heavier. As a result, the downward flows along the vertical centerline are originated, while the lighter fluid will rise, cooling as it moves. Consequently, the circulation flow pattern is generated. The clockwise and counter-clockwise circulations are located respectively on the left side and right side within the enclosure. The circulations get larger and expand downward with time. An increase in strength of the vortices develops fast during early simulation times, and its maximum magnitude reaches 6.0. Subsequently the vortices are weakened. Similarly, temperature distribution progressively evolves relatively fast in the early times. Slow evolution is observed after that. This result corresponds well with the decrease in strength of flow circulations. Unlike the cooling case, in which a presence of negative density mainly causes an unstable condition, in the heating case the lateral density gradient near the top surface is the only cause to the unstable condition that actually leads to the buoyancy force. This reason explains why the heated circulations are weaker than the cooled circulations presented earlier. This is because of large/strong viscous effects. It is evident from figures 3 and 9 that the cooling case reveals a considerably faster thermal evolution thereby greater convection rate. Furthermore, heat transfer in the vertical direction is much greater than that in the span wise direction.

Figure 10 shows the roles of Rayleigh number on heat transfer mechanism/behavior. Various Rayleigh numbers (Ra = 5×10^3 , 10^4 , 5×10^4 and 10^5) are examined whereas the Darcy number of 0.1, porosity of 0.8, and h of 60 w/m²K are fixed. The Rayleigh number provides the ratio of buoyancy forces to change in viscous forces.

As Rayleigh number increases, the buoyancy-driven circulations inside the enclosure become stronger as seen from greater magnitudes of stream function. For large Ra (Ra = 5×10^4 and 10^5), contour lines of temperature penetrate faster relative to the low Ra case especially near the central locations. The result is more pronounced for larger Ra. This incident results from strong flow in the downward direction around the central domain. The downward flows assist heat to transfer towards the bottom of the enclosure. In contrast, near the vertical walls where the upward flows are present, the thermal propagation is hindered.

Effects of the Darcy number on the fluid flow and temperature inside the rectangular cavity are depicted in figure 11. The contour of isotherms and streamlines are plotted for different Darcy numbers while ε , Pr and h are kept at 0.8, 1.0 and 60 w/m²K respectively. Relatively high Ra of 5×10⁴ is chosen. The Darcy number, which is directly proportional to the permeability of the porous medium, was set to 0.001, 0.01 and 0.1. The case in which the porous medium is absent corresponds to infinite Darcy number. The presence of a porous medium within rectangular enclosure results in a force opposite to the flow direction which tends to resist the flow which corresponds to suppress in the thermal currents of the flow as compared to a medium with no porous (infinite Darcy number). It is evident that the increase in Da enhances the streamline intensities thereby assisting downward flow penetration, which causes the streamline lines, i.e., two symmetrical vortices to stretch further away from the top surface. This results in expanding the region for which the convection significantly influences an overall heat transfer process. Further, the evolution results reveal faster rate of vertical temperature distribution than lateral rate. The results are consistent with the thermal behaviors observed in figure 10 for the same reasoning, which confirms how a flow direction impacts the convection heat transfer. On the other hand, as the Darcy number decreases, the flow circulations as well as thermal penetration are progressively suppressed due to the reduced permeability of the medium. Figure 11d (Da = 0.001) indicates that as Darcy number approaches zero, the two circulations confined within the top domain appear very weak. In the remaining area, the fluid is nearly stagnant with very small temperature gradient suggesting that conduction is dominant due to minimal flow activities.

Figure 12 presents how the average Nusselt number changes with time for a variety of Rayleigh numbers. The local Nu at the open portion on the top boundary is computed according to equation (16). The average Nusselt number \overline{Nu} is then obtained, based on

equation (17). Initially, the value of $\overline{\text{Nu}}$ decreases rapidly for all cases of Rayleigh numbers, clearly due to the fast reduction of temperature gradients. In the case of low Rayleigh number of $2x10^4$, $\overline{\text{Nu}}$ progressively decreases with time. While for higher Ra $(5x10^4, 8x10^4)$, $\overline{\text{Nu}}$ values become greater and reach peak values after some time. Further increasing Ra $(8x10^4)$, higher maximum Nu is reached more quickly due to greater flow intensities. At late simulation times when stable state is approached, the values of $\overline{\text{Nu}}$ continually decrease and essentially level off at late times, thereby diminishing heat transfer by means of heat convection. It can be expected that $\overline{\text{Nu}}$ will continue to decrease with time as the steady state is reached.

To gain insights into the observation made, the local values of the corresponding thermal and flow behaviors were traced for Ra of $8x10^4$. The data are extracted and depicted in figure 13 at τ of 0.02, 0.1 and 0.16. The streamlines and isotherms are illustrated in figure 13a-c at $\tau=0.02$, 0.1 and 0.16 respectively. At $\tau=0.02$, the averaged Nu is small due to minimal flow activities. Then $\overline{\text{Nu}}$ gets higher as the flows gets stronger, which can be seen in figure 13(b) at $\tau=0.1$. The effect of the rigorous flows overcomes the continual reduction of temperature gradient, resulting in the increase in $\overline{\text{Nu}}$. At the subsequent times, the viscous effect increasingly weakens the flows as shown in figure 13(c). As a result, the reduction of temperature gradient prevails, causing $\overline{\text{Nu}}$ to decrease. These results correspond well with the variation with time of the averaged Nu, depicted in figure 12. The results confirm the validation of the proposed formulation of Nu.

To better understand the effects of Darcy number on the heat transfer behavior, variations of $\overline{\text{Nu}}$ with time for different Darcy number are shown in figure 14. The resulting plots show an interesting evidence of similar variations of $\overline{\text{Nu}}$ on Da and those on Ra, which was observed previously in figure 12. Average Nu correlates with Ra in a way similar to correlation of Nu with Da. Further increasing values of Da (0.05 and 0.1) cause larger $\overline{\text{Nu}}$ variations. Locations of the peak values are altered relative to Da value. A peak of profile is reached more quickly for higher Da. Greater Da gives higher $\overline{\text{Nu}}$, suggesting that the higher overall heat transfer rate is due to more energetic vortices. However, $\overline{\text{Nu}}$ substantially reduces at late times.

5. Conclusions

Numerical simulations of natural convection flow through a fluid-saturated porous medium in a rectangular cavity due to convection at top surface were performed. Transient effects of associated controlling parameters were examined. The twodimensional flow is characterized mainly by two symmetrical eddies that are initiated by the presence of buoyancy effect. In the cooling case, the buoyancy effect is associated not only with the lateral temperature gradient at locations near the top surface, but also with the condition that the density gradient is negative in the direction of gravitational force. On the other hand, the buoyancy force is induced solely by the lateral temperature gradient in the heating case. The cooling and heating flow directions are opposite. Cooling flows are much stronger due to greater buoyancy effects, indicating higher overall convection rate. The heat transfer mechanism is analyzed using the newly derived formulation of Nu which captures the heat transfer behaviors reasonably. Heat transfer rate is faster around vertical symmetric line relative to the near-wall regions. Large values of Rayleigh number increase streamline intensities, thus enhancing the downward flow penetration. The temperature stratification penetrates deeper toward the bottom wall, and temperature range within the domain is extended. Therefore it enlarges the region where convection mode is significant. Small values of Darcy number hinder the flow circulations. Therefore the heat transfer by convection is considerably suppressed. Moreover, the dependences of Nu on Da and on Ra are found to have the same trends.

References

- [1] Al-Amiri, A.M., (2000). Analysis of Momentum and Energy Transfer in a Lid-Driven Cavity Filled with a Porous Medium. International Journal of Heat and Mass Transfer, 43, 3513-3527.
- [2] Al-Amiri, A.A., (2002). Nature convection in porous enclosures: The application of the two-energy equation model, Numerical Heat Transfer Part A, 41, 817-834.
- [3] Aydin, O., (2000). Determination of Optimum Air-Layer Thickness in Double-Pane Windows. Energy and Buildings, 32, 303-308.
- [4] Basak, T., Roy, S., Paul, T., Pop, I., (2006). Natural convection in a square cavity filled with porous medium: Effects of various thermal boundary conditions. International Journal of Heat and Mass Transfer, 49, 1430-1441.

- [5] Beckermann, C., Viskanta, R., Ramadhyani, S., (1986). A numerical study of non-Darcian natural convection in a vertical enclosure filled with a porous medium. Numerical Heat Transfer, 10, 557-570.
- [6] Bera, P., Eswaran, V., Singh, P., (1998). Numerical study of heat and mass transfer in an anisotropic porous enclosure due to constant heating and cooling. Numerical Heat Transfer Part A, 34, 887-905.
- [7] Bera, P., Khalili, A., (2002). Double-diffusive natural convection in an anisotropic porous cavity with opposing buoyancy forces: multi-solutions and oscillations. International Journal of Heat and Mass Transfer, 45, 3205-32.
- [8] Bergman, T.L., Incropera, F.P., Viskanta, R., (1986). Correlation of Mixed Layers Growth in Double-Diffusive, Salt-Stratified System Heated from Below. Journal of Heat Transfer, 108, 206-211.
- [9] Bilgen, E., Mbaye, M., (2001). Be'nard cells in fluid-saturated pourous enclosures with lateral cooling. International Journal of Heat and Fluid Flow, 22, 561-570.
- [10] Brinkmann, H.C., (1947). On the permeability of media consisting of closely packed porous particles. Applied Sciences Research, 1, 81-86.
- [11] Bradean, R., Ingham, D.B., Heggs P.J., Pop, I., (1997). The unsteady penetration of free convection flows caused by heating and cooling flat surfaces in porous media. International Journal of Heat and Mass Transfer, 40, 665-687.
- [12] Cheng, P., (1978). Heat transfer in geothermal systems. Advances in Heat Transfer, 4, 1-105.
- [13] El-Refaee, M. M., Elsayed, M.M., Al-Najem, N.M., Noor, A.A., (1998). Natural convection in partially cooled tilted cavities. International Journal of Numerical Methods, 28, 477-499.
- [14] Imberger, J., Hamblin, P.F., (1982). Dynamics of Lakes, Reservoirs, and Cooling Ponds. Annual Review of Fluid Mechanics, 14, 153-187.
- [15] Khanafer, K.M., Chamkha, A.J., (1998). Mixed Convection Flow in a Lid-Driven Enclosure Filled with a Fluid-Saturated Porous Medium. International Journal of Heat and Mass Transfer 42, 2465-2481.
- [16] Khanafer, K., Vafai, K., (2002). Double-Diffusive Mixed Convection in a Lid-Driven Enclosure Filled with a Fluid-Saturated Porous Medium. Numerical Heat Transfer Part A, 42, 465-486.
- [17] Lauriat, G., and Prasad, V., (1987). Natural convection in a vertical porous cavity: a numerical study for Brinkmann-extended Darcy formulation. ASME Journal of Heat Transfer, 109, 295-320.

- [18] Lauriat, G., Prasad, V., (1989). Non-Darcian effects on natural convection in a vertical porous enclosure. International Journal of Heat and Mass Transfer, 32, 2135-2148.
- [19] Mohammad, A.A., (2000). Nonequilibrium natural convection in a differentially heated cavity filled with a saturated porous matrix. Journal of Heat Transfer, 122, 380-384.
- [20] Nield, D.A., Bejan, A., (1999). Convection in Porous Media, Springer, New York.
- [21] Nithiarasu, P., Seetharamu, K.N., Sundararajan, T., (1997). Natural convective heat transfer in a Fluid Saturated variable porosity medium. International Journal of Heat and Mass Transfer, 40, 3955-3967.
- [22] Nithiarasu, P., Seetharamu, K.N., Sundararajan, T., (1998). Numerical Investigation of Buoyancy Driven Flow in a Fluid Saturated non-Darcian Porous Medium. International Journal of Heat and Mass Transfer, 42, 1205-1215.
- [23] Oosthuizen P.H., Patrick, H., (1995). Natural Convection in an Inclined Square Enclosure Partly Filled with a Porous Medium and with a Partially Heated Wall, American Society of Mechanical Engineers. Heat Transfer Division, (Publication) HTD 302, 29-42.
- [24] Oztop, H.F., (2007). Natural convection in partially cooled and inclined porous rectangular enclosure. International Journal of Thermal Sciences, 46, 149-156.
- [25] Pakdee, W., Rattanadecho, P., (2006). Unsteady effects on natural convective heat transfer through porous media in cavity due to top surface partial convection Applied Thermal Engineering. 26, 2316-2326.
- [26] Pop, I., D.B. Ingham, D.B., (2001). Convective Heat Transfer, Mathematical and Computational Modeling of Viscous Fluids and Porous Media, Pergamon, Oxford.
- [27] Ratanadecho, P., Aoki, K., Akahori, M., (2001). A Numerical and Experimental Investigation of the Modeling of Microwave Drying Using a Rectangular Wave Guide. Journal of Drying Technology, 19, 2209-2234.
- [28] Ratanadecho, P., Aoki, K., Akahori, M., (2002). Influence of Irradiation Time, Particle Sizes and Initial Moisture Content During Microwave Drying of Multi-Layered Capillary Porous Materials. ASME Journal of Heat Transfer, 124, 151-161.
- [29] Stanish, M.A., Schager, G.S., Kayihan, F., A., (1986). Mathematical Model of Drying for Hygroscopic Porous Media. AIChE Journal, 32, 1301-1311.
- [30] Tong, T.W., Subramanian, E., (1985). A boundary-layer analysis for natural convection in vertical porous enclosures-use of the Brinkman-extended Darcy model, ASME Journal of Heat Transfer, 28, 563-571.
- [31] Vafai, K., (2000). Handbook of Porous Media, Marcel Dekker, New York

TABLES AND FIGURES .

TABLES

Table 1. Comparison of the results obtained in the present study with those of Aydin [3].

	Present work	Published work [3]	Difference (%)
ψ _{max}	5.070	5.087	0.33
U_{max}	16.300	16.225	0.46
V _{max}	19.730	19.645	0.43

Table 2. Comparison of the results obtained in the present study with those of Nithiarasu et al. (1997). (Da=0.01, Ra = 10^3 , porosity = 0.6)

	Present work	Published work [8]	Difference (%)
Ψ _{m2x}	2.53	2.56	1.17
$V_{\rm max}$	9.49	9.34	1.60

LIST of FIGURE CAPTIONS

- Fig 1. Schematic representation of the computational domain.
- Fig 2. Test results for validation purpose: (a) previously published results [19] (b) present numerical simulation.
- Fig 3. Sequential files for contours of temperature and streamlines at times $\tau = 0.0125$,
- 0.09, 0.1675, and 0.2475. (Ra = 10^4 , Da = 0.01, Pr = 1.0, $\epsilon = 0.8$, and h = $100 \text{ W/m}^2\text{K}$)
- Fig 4. Contours of temperature and streamlines (a) $h = 60 \text{ W/m}^2\text{K}$ (b) $h = 300 \text{ W/m}^2\text{K}$. (Ra = 10^4 , Da = 0.1, Pr = 1.0, and $\varepsilon = 0.8$)
- Fig 5. Contours of temperature and streamlines (a) Da = infinity (b) Da = 0.1 (c) Da = .001. (Ra = 10^4 , h = $60 \text{ W/m}^2\text{K}$, Pr = 1.0, and $\varepsilon = 0.8$)
- Fig 6. Temperature distribution contours within a medium in the absent of porous (solid line) overlaid by the temperature distribution contours in a porous medium with Da of 0.001 (dash line). Data is taken from that of Fig 5.
- Fig 7. Contours of temperature and streamlines (a) Ra = 10^3 (b) Ra = 10^4 (c) Ra = 10^5 . (Da = 0.1, h = 60 W/m²K, Pr = 1.0, and ε = 0.8)
- Fig 8. Temperature distribution contours within a porous medium with $Ra = 10^3$ (dash line) overlaid by the temperature distribution contours in a porous medium with $Ra = 10^5$ (solid line). Data is taken from that of Fig 7.
- Fig 9. Sequential files with the cooling boundary for contours of temperature and streamlines at times $\tau = (a)~0.013$, (b) 0.088, (c) 0.168, and (d) 0.245. (Ra = 5×10^4 , Da = 0.1, Pr = 1.0, $\epsilon = 0.8$, and $h = 60 \text{ W/m}^2\text{K}$)
- Fig 10. Contours of temperature and streamlines for the cooling case (a) $Ra = 5x10^3$ (b) $Ra = 10^4$ (c) $Ra = 5x10^4$ (d) $Ra = 10^5$. (Da = 0.1, h = 60 W/m²K, Pr = 1.0, and $\varepsilon = 0.8$)

Fig 11. Contours of temperature and streamlines for the cooling case (a) Da = infinity (b) Da = 0.1 (c) Da = 0.01 (d) Da = 0.001. (Ra = 5×10^4 , h = $60 \text{ W/m}^2\text{K}$, Pr = 1.0, and ε = 0.8)

Fig 12. Variations of the average Nusselt number with time for different Rayleigh numbers. (Da = 0.01, h = 60 W/m²K, Pr = 1.0, and ε = 0.8)

Fig 13. (a)-(c) temperature contours overlaid by velocity vectors at $\tau = 0.02$, 0.1 and 0.16 respectively. Data is taken from that of figure 7 for Ra = 8×10^4 .

Fig 14. Variations of the average Nusselt number with time for different Darcy numbers. (Ra = 5×10^4 , h = $60 \text{ W/m}^2\text{K}$, Pr = 1.0, and $\varepsilon = 0.8$)

FIGURES

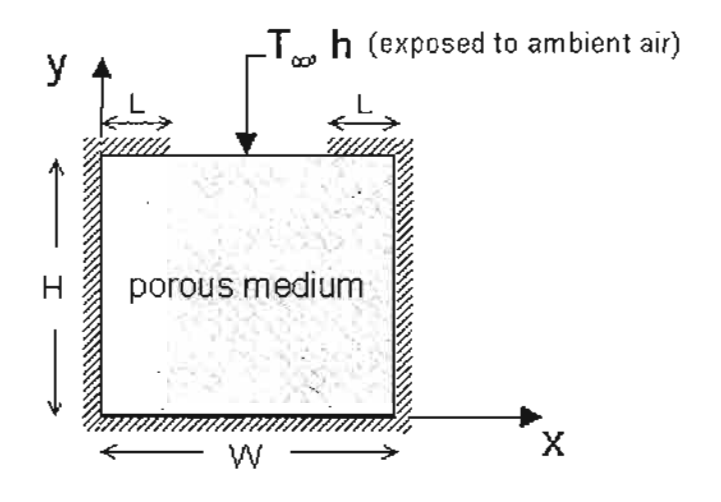
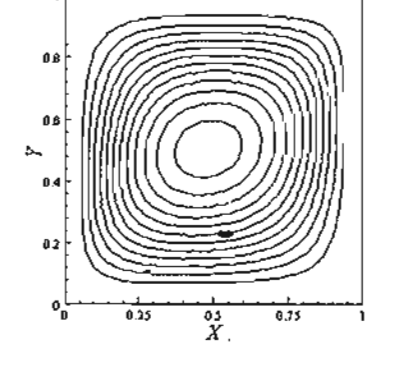


Fig 1

(a)



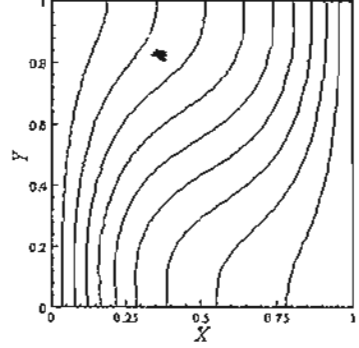


Fig 2

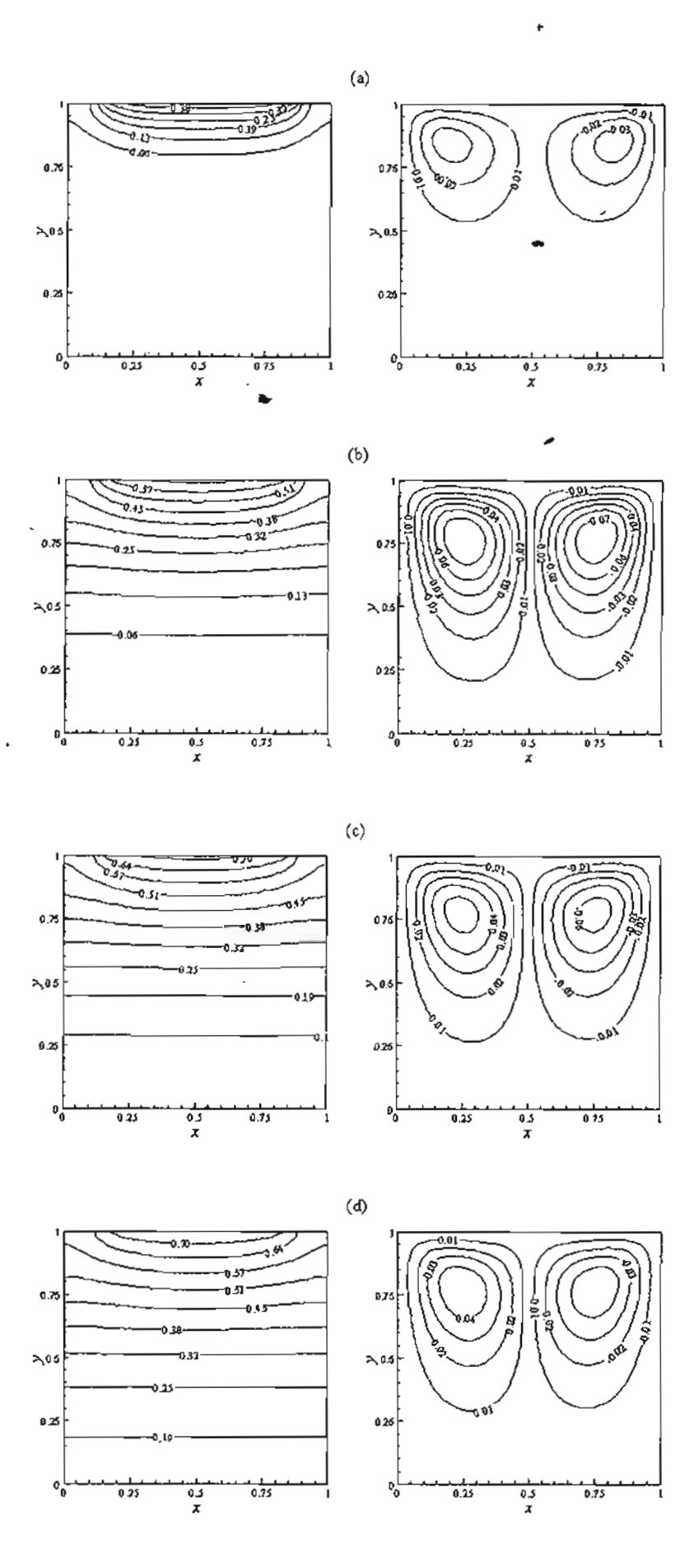


Fig 3

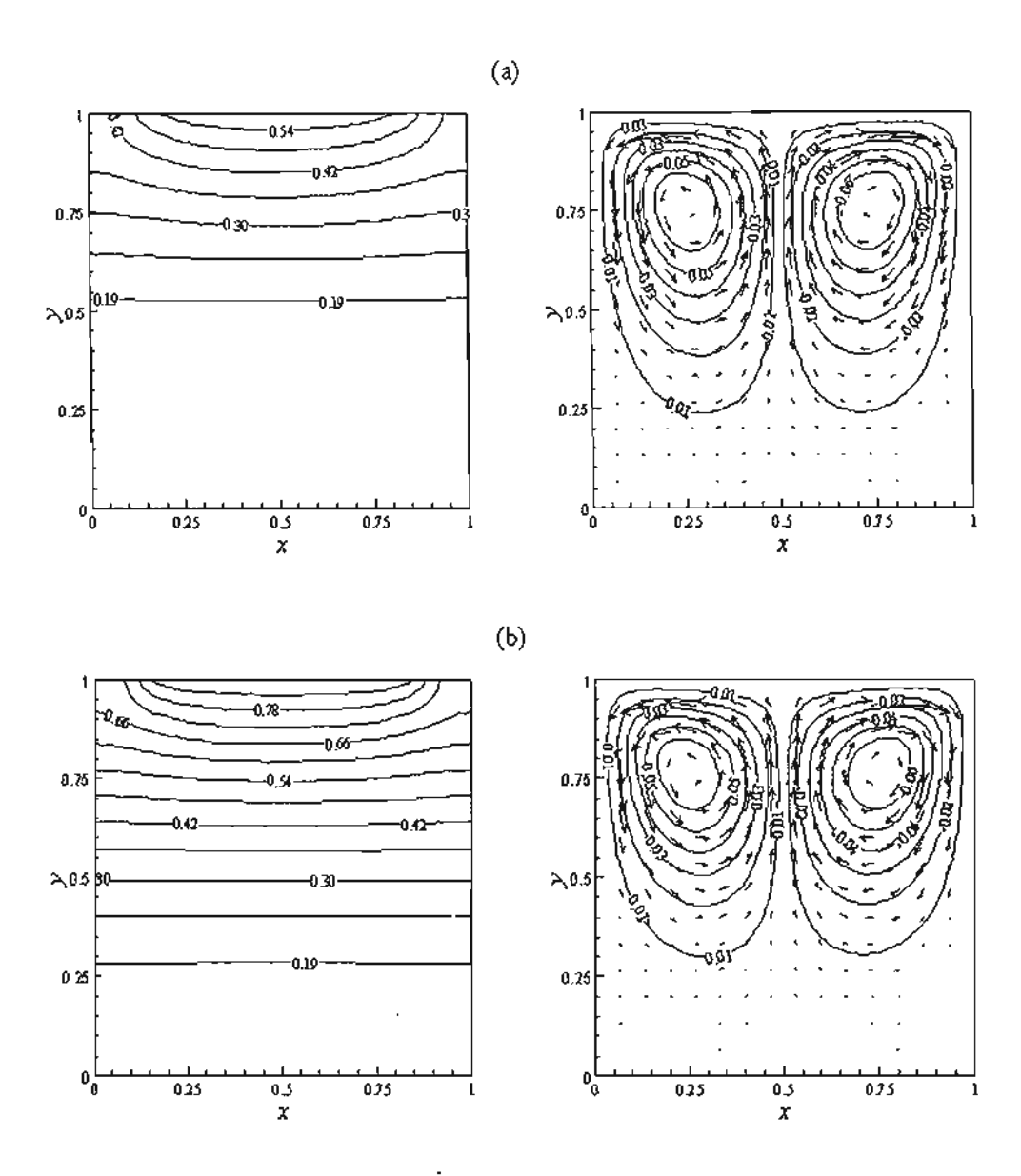


Fig 4

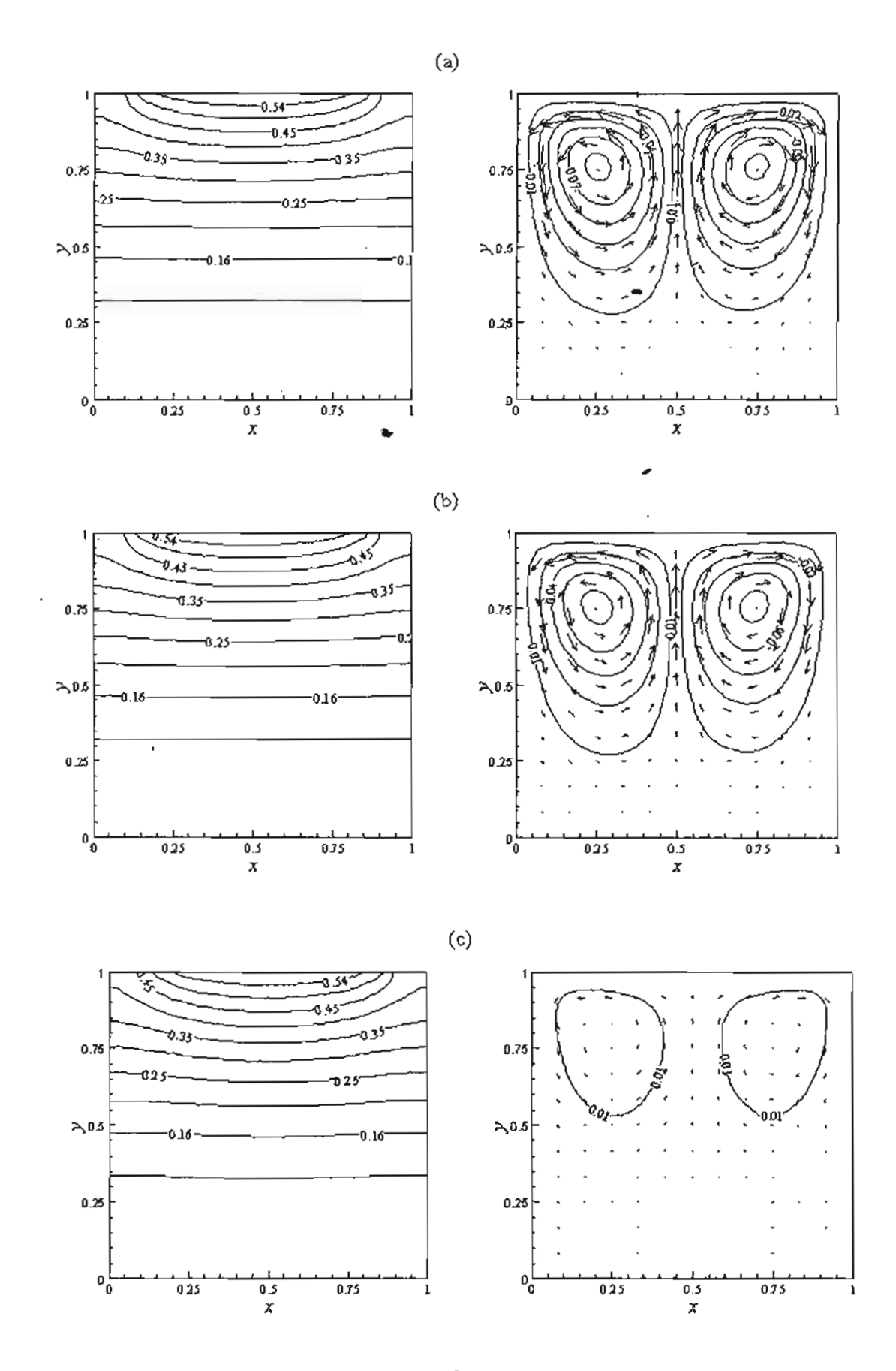


Fig 5

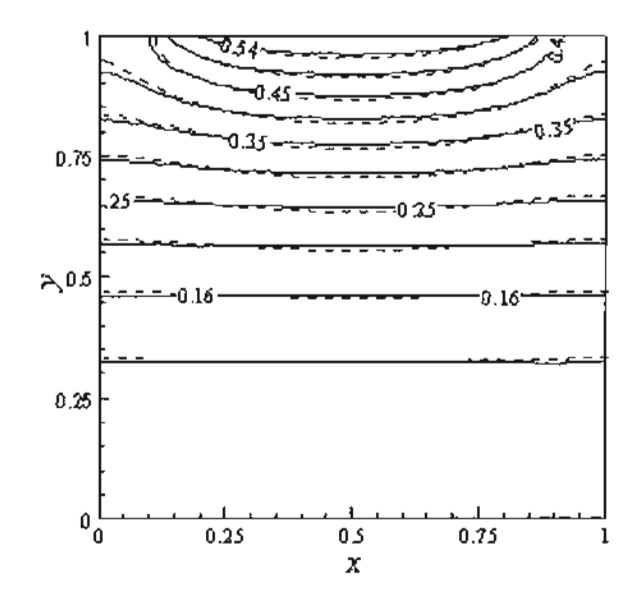


Fig 6

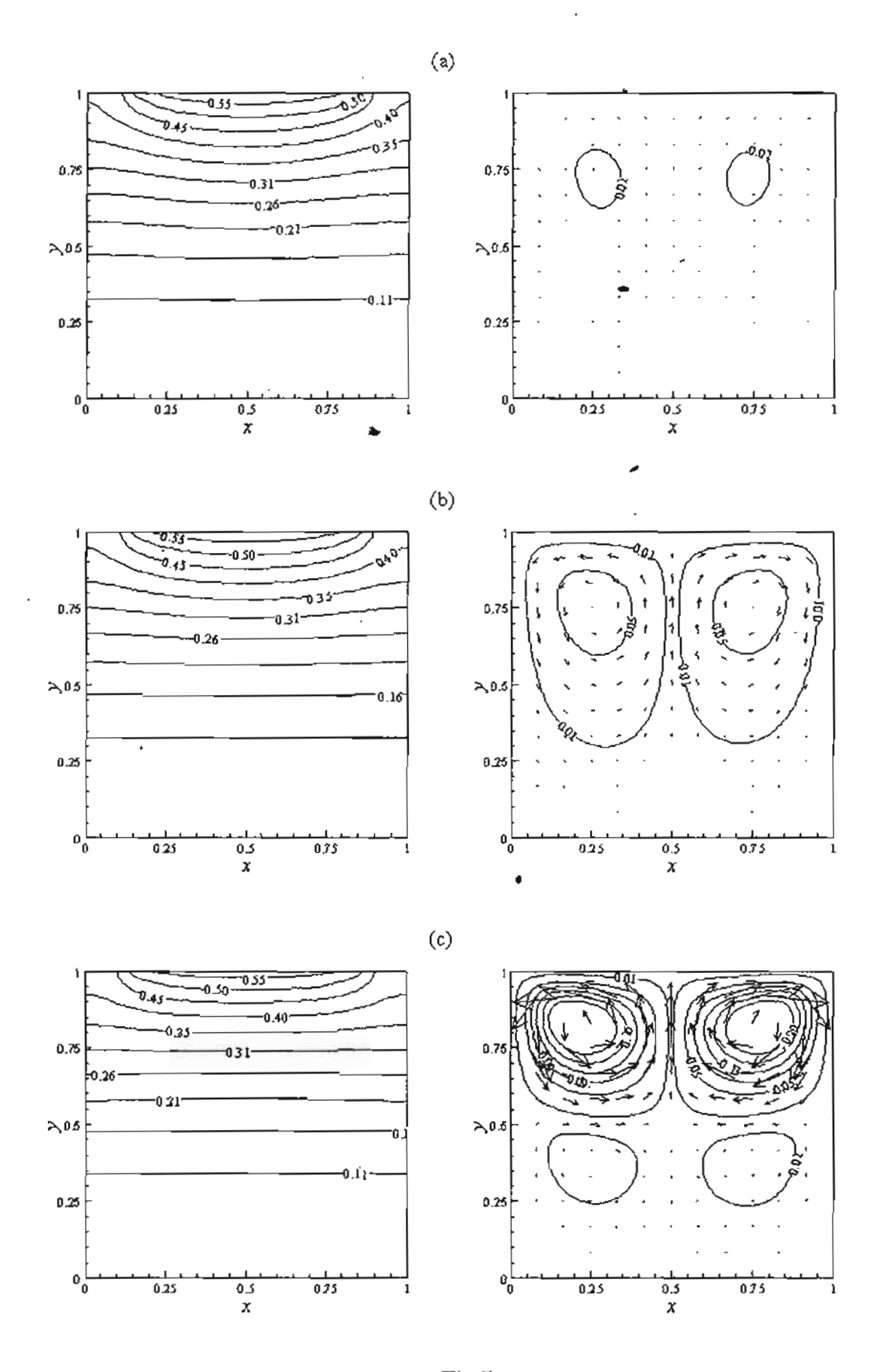


Fig 7

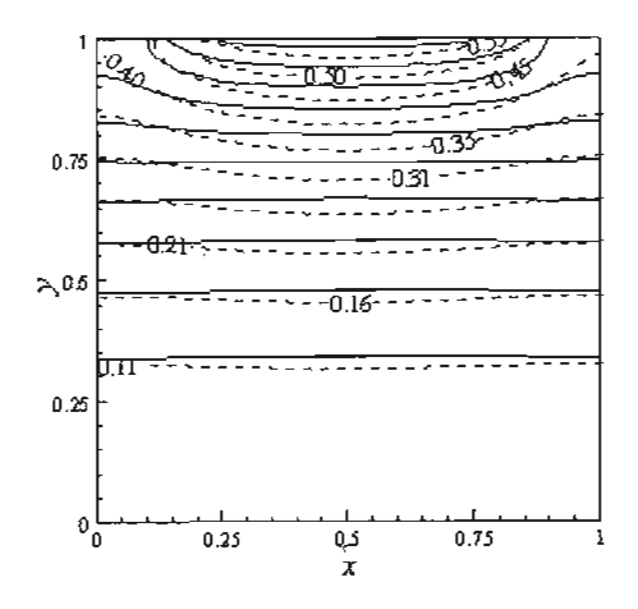


Fig 8

35

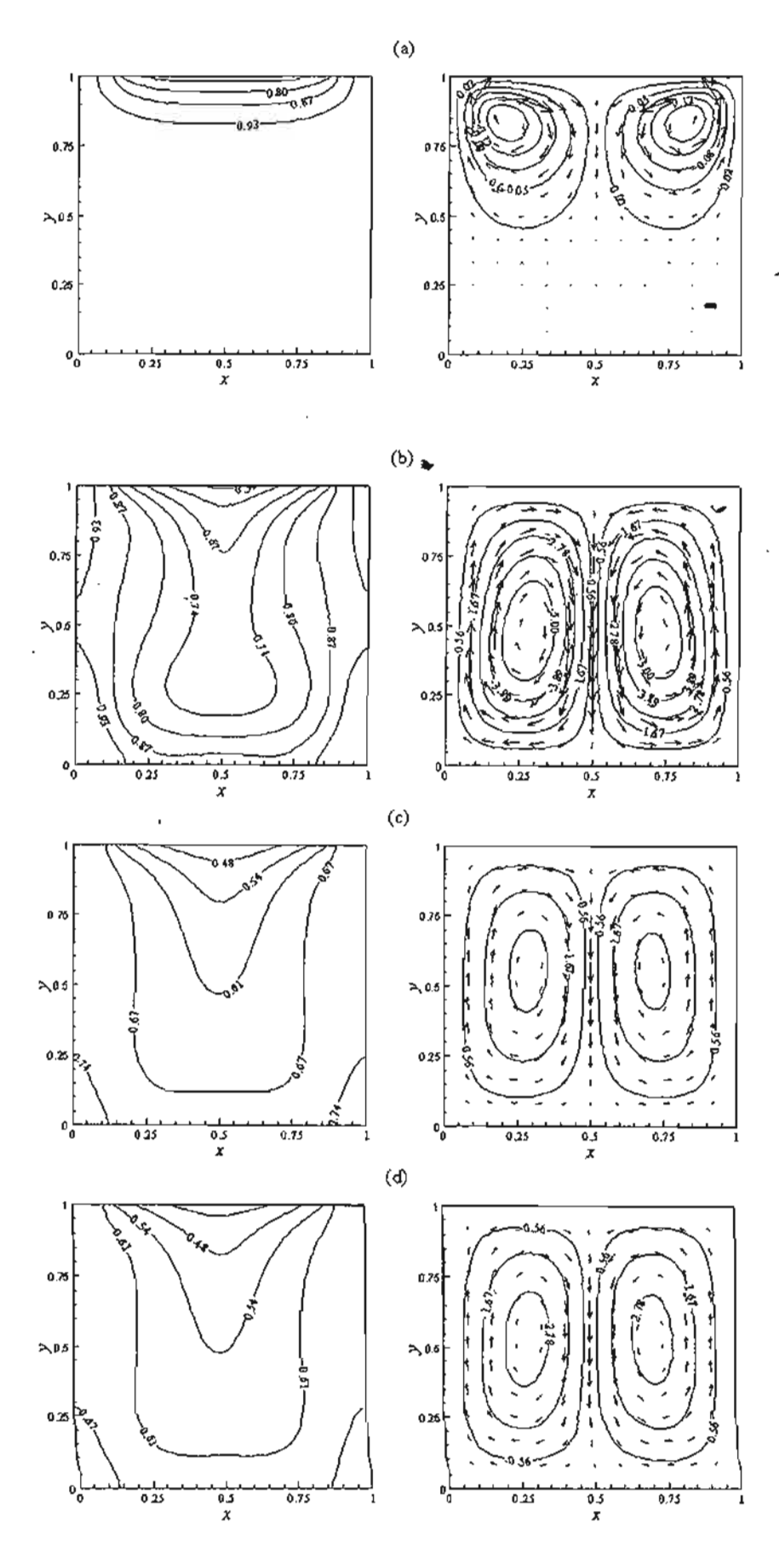


Fig 9

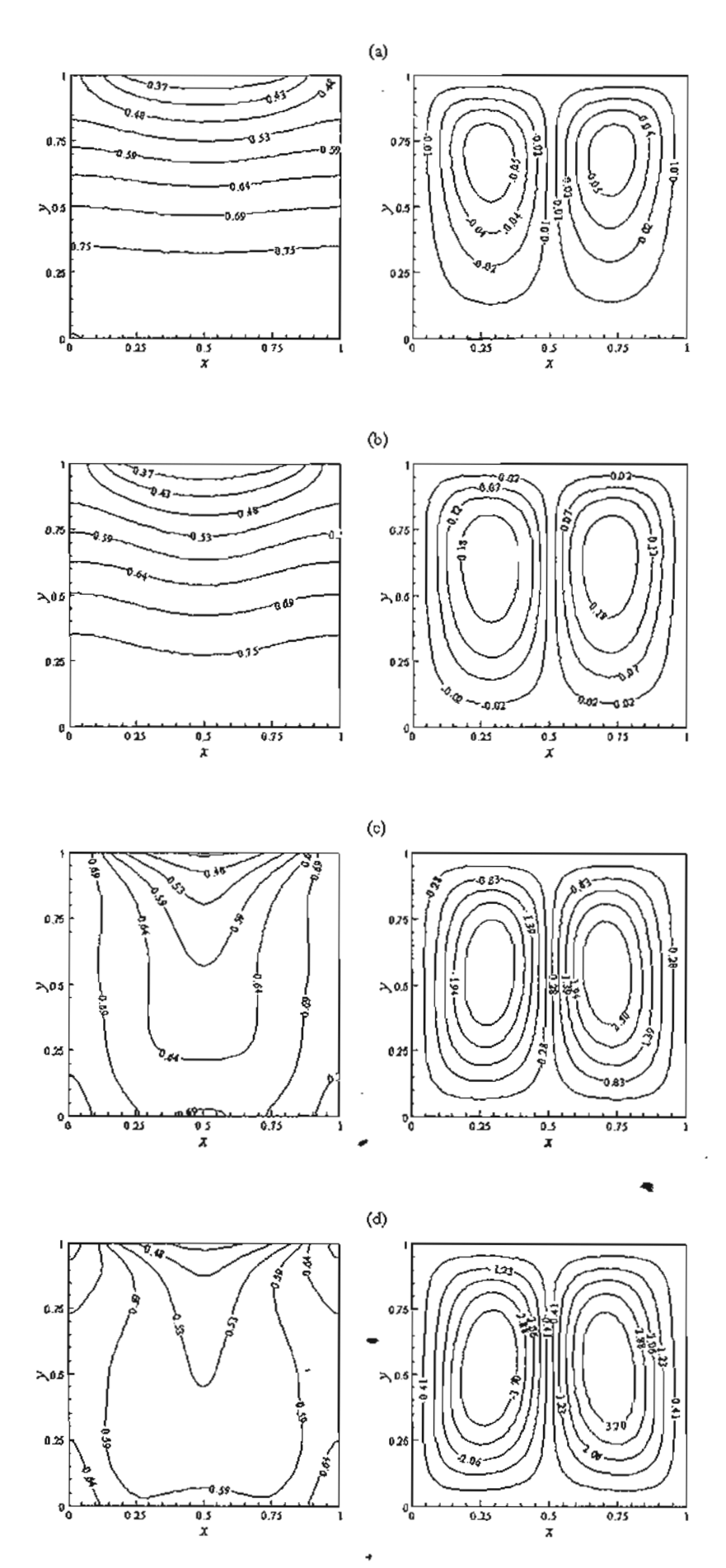


Fig 10

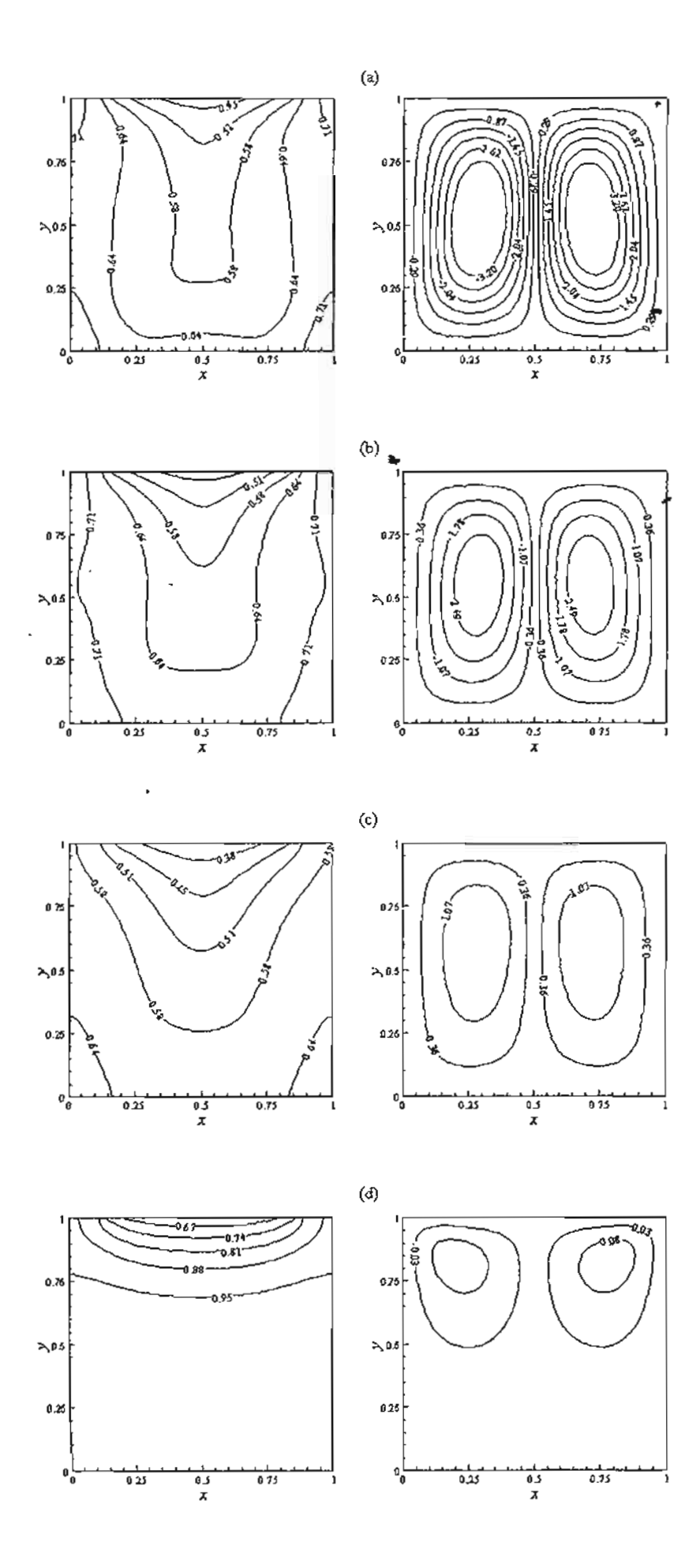


Fig 11

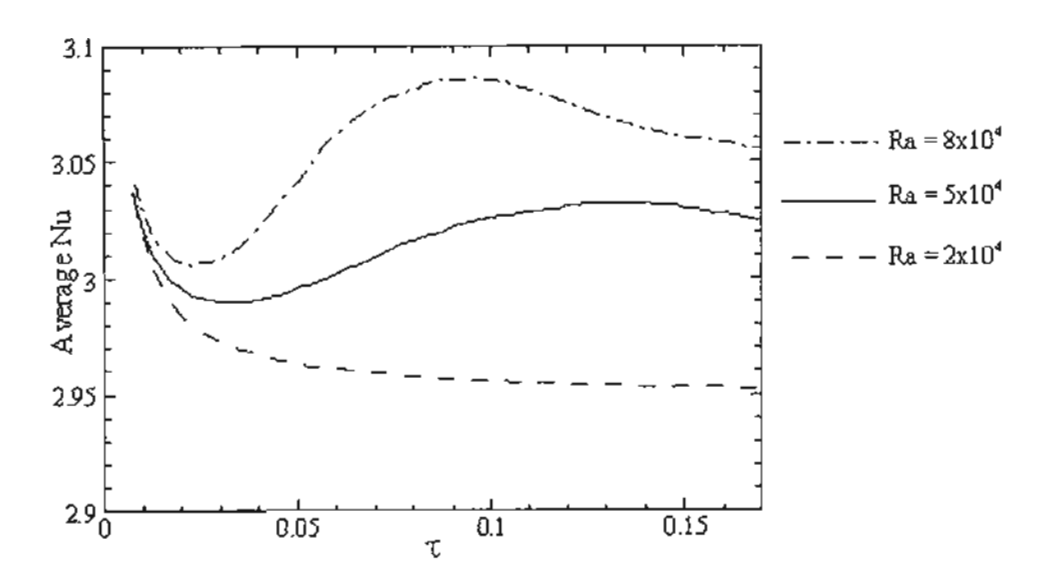


Fig 12

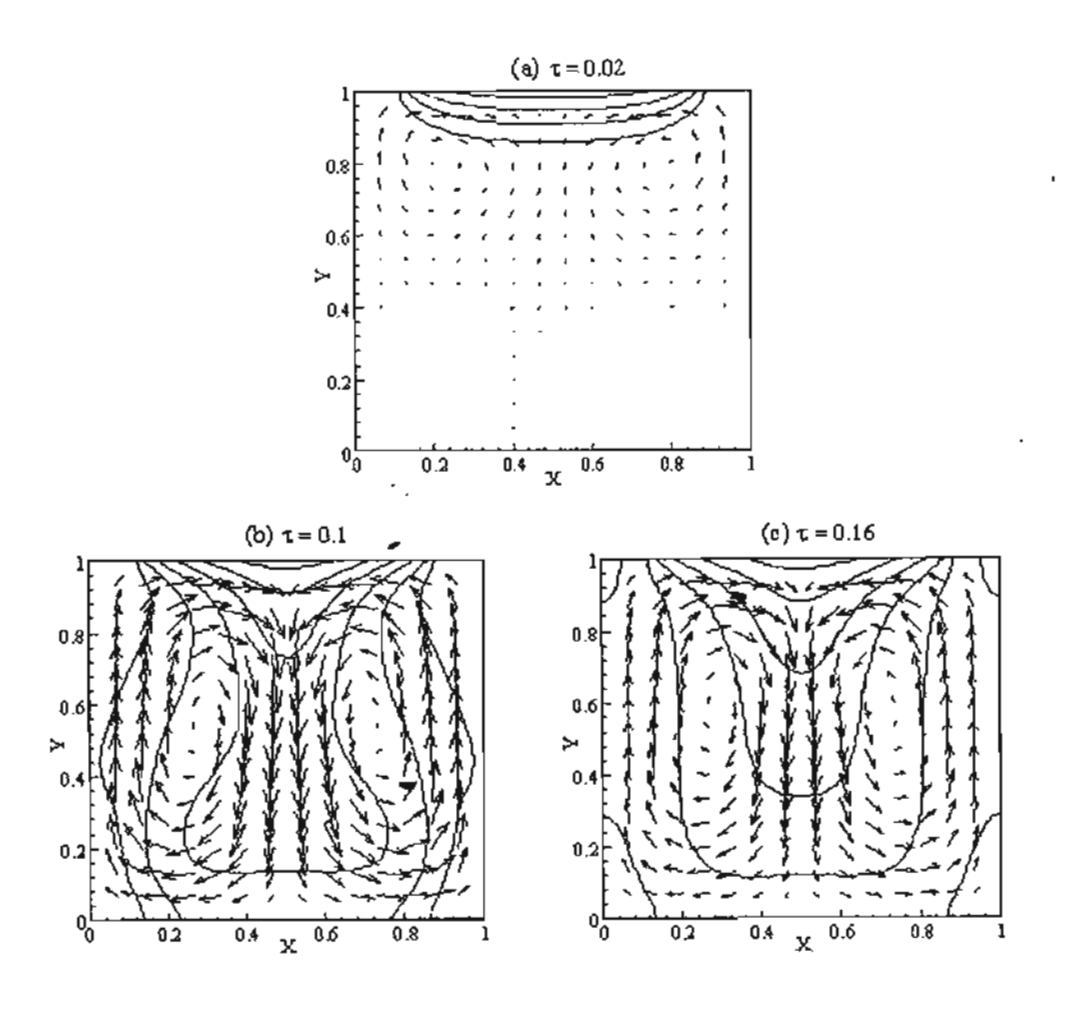


Fig 13

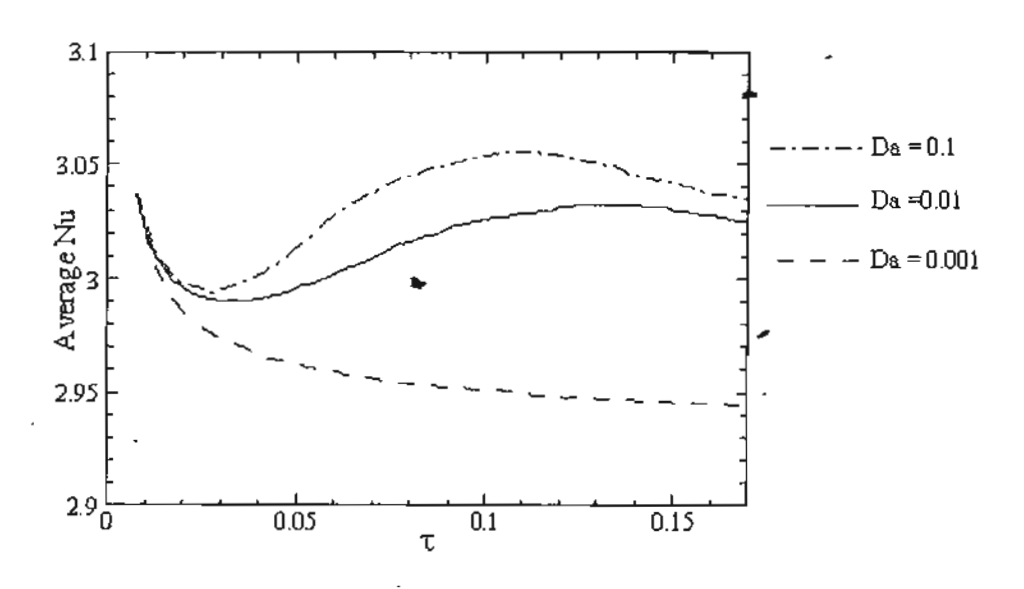


Fig 14

2.2 Analysis of Microwave Heating of Dielectric Materials Using a Rectangular Wave Guide

1. Introduction

Microwave heating is one of the most interesting methods for heating materials. Unlike other heat sources such as conventional heating, where heat is applied externally to the surface of the material, microwave irradiation penetrates and simultaneously heats the bulk of the material. Microwave technology has several advantages over conventional mechanical methods, such as minimizing the heating times, uniform temperature distribution, high energy efficiency, and offers improvements in product quality for various industrial fields. Many successful examples of this application, including the drying of foods, drying of textiles, freeze drying process, and vulcanizations of rubber.

The reader is referred to Metaxas and Meredith [1] and Saltiel and Datta [2] for an introduction to heat and mass transfers in microwave processing. Other important papers addressing modeling of microwave heating processes include Ayapa et al. [3], Clemens et al. [4], Dibben et al. [5], Zhao et al. [6], Bows et al. [7], Zhao et al. [8], Watanuki [9], Basak and Basak et al. [10] and Ratanadecho et al. [11-13].

Although most of previous investigations considered simulations of microwave heating in solid sample, a little effort has been reported on study of multi-dimensional heating process of liquid layer by microwave fields. Moreover, full comparison between numerical results with experimental heating data is found very rare.

A study of microwave heating of liquid was investigated by many researchers. A study of natural convection in a liquid expose to microwave was studied by Datta et al. [2] which the microwave power absorbed was assumed to decay exponentially into the sample following the aid of Lambert's law. However, this assumption is valid only for the large sample dimensions and high loss dielectric materials. The important paper addressing modeling of microwave driven convection in square cavity exposed to waves from different directions was made by Ayapa et al. [3]. A study of microwave induced natural convection in 3D was made by Zhang, Jackson, and Ungan (2000). The model solved the Maxwell's equation in 3D using the FDTD method and solved the flow field for distilled water and corn oil. Ratanadecho et al. [13] were the first who investigated, numerically and experimentally, for microwave heating of liquid layer with different dielectric properties using a rectangular wave guide. The

movement of liquid induced by microwave energy was taken into account. Coupled electromagnetic, hydrodynamic and thermal field were simulated in two dimensions. The spatial variation of electromagnetic field was obtained by solving Maxwell's equations with the FDTD method. Their work demonstrated the effects of microwave power level and liquid dielectric properties on the degree of penetration and rate of heat generation within the liquid layer. The simulated results were validated by comparing with experimental results. Recently, microwave heating of liquid flowing in a rectangular duct passing through the cubic cavity was study by Zhu et al. [14]. The effects of the diameter of applicator tube and the shape of microwave cavity were investigated. The microwave heating of liquid inside rotating container was numerically study by Chatterjee et al. [10], in which, the effects of the various parameters, namely the rotational forces, power source intensity and the gravitational forces, on the microwave heating of containerized liquids in the presence of rotating turntables were investigated.

However, except in the studies by Ratanadecho et al. [11]-[13], a little effort has been reported on experimental study of microwave heating of liquid layer or microwave heating of a fluid-saturated porous packed bed in detail. Due to the limited amount of theoretical and experimental work on microwave heating of dielectric materials, i.e., liquid layer and fluid-saturated porous packed bed reported to date, the various effects are not fully understood and numbers of critical issues remain unresolved. These effects of reflection rate of microwave, the variation of microwave power level, dimension and location of sample and dielectric properties during microwave heating of dielectric materials have not been systematically studied. Generally the variation of the microwave power level, dimension and location of sample and change of dielectric properties during microwave heating of dielectric materials could change the degree of penetration and rate of heat generation within the heating layer. The reflection rate of microwave strongly depends on the dielectric properties of the heating layer so that the effects of the variation of microwave power level, dimension and location of sample and dielectric properties and must be considered in this work.

This study reports an experimental data during microwave heating of dielectric materials i.e., liquid layer and saturated porous packed bed using a rectangular

waveguide in which the microwave of TE_{i0} mode operating at a frequency of 2.45GHz is employed.

2. Related Theories

With the basic knowledge of heating by microwave energy, it concerns heat dissipation and typical microwaves propagation the basic equation to calculate the density of microwave power absorbed by dielectric material (Q) can be here below established [22].

$$Q = \omega \varepsilon_0 \varepsilon_0^* E^2 = 2\pi . f . \varepsilon_0 . \varepsilon_0^* (\tan \delta) E^2$$
 (1)

where E is electromagnetic field intensity; f is microwave frequency; ω is angular velocity of microwave; ε_{i} is relative dielectric constant; ε_{0} is dielectric constant of air and $\tan \delta$ is dielectric loss tangent coefficient.

From equation (1), Q is directly proportional to the frequency of the applied electric field and dielectric loss tangent coefficient and root-mean-square value of the electric field. It means that increasing of $\tan \delta$ of sample, absorption of microwave energy and generated heat are also increased. While $\tan \delta$ is small, microwave will penetrate into sample without heat generation. However the temperature increasing is probably depending on other factors such as specific heat, size and characteristic of sample.

When the material is heated unilaterally, it is found that as the dielectric constant and loss tangent coefficient vary, the penetration depth will be changed and the electric field within the dielectric material is altered. The penetration depth is used to denote the depth at which the power density has decreased to 37 % of its initial value at the surface [14].

$$D_{\rho} = \frac{1}{2\pi f} \sqrt{\frac{\varepsilon_{r} \left(\sqrt{1 + \left(\frac{\varepsilon_{r}}{\varepsilon_{r}}\right)^{2}} - 1\right)}{\frac{2\pi f}{\upsilon}}} = \frac{\frac{1}{2\pi f} \sqrt{\frac{\varepsilon_{r} \left(\sqrt{1 + \left(\tan \delta\right)^{2}} - 1\right)}{2}}}{\frac{2\pi f}{\upsilon} \sqrt{\frac{\varepsilon_{r} \left(\sqrt{1 + \left(\tan \delta\right)^{2}} - 1\right)}{2}}}$$

(2)

where D_{ρ} is penetration depth ε_{ρ} is relative dielectric loss factor and v is microwave speed. The penetration depth of the microwave power is calculated according to equation (2), which shows how it depends on the dielectric properties of the material. It is noted

that products with huge dimensions and high loss factors, may occasionally overheat a considerably thick layer on the outer layer. To prevent such phenomenon, the power density must be chosen so that enough time is provided for the essential heat exchange between boundary and core. If the thickness of the material is less than the penetration depth, only a fraction of the supplied energy will become absorbed. In example, consider the dielectric properties of water typically show moderate lossiness depending on the temperature. The water layer at low temperature typically shows slightly greater potential for absorbing microwaves. In the other words, an increase in the temperature typically decreases ε_r , accompanied by a slight increment in D_p .

3. Experimental apparatus

In the present study, the experimental analysis of heat transfer in dielectric material is conducted. Fig. 1(a) shows the experimental apparatus. The microwave system is a monochromatic wave of TE10 mode operating at a frequency of 2.45 GHz. Microwave is generated by magnetron, it is transmitted along the z-direction of the rectangular wave guide with inside dimensions of 110 mm x 54.61 mm² toward a water load that is situated at the end of the wave guide (Fig. 1(b)). The water load (lower absorbing boundary) which ensures that only a minimal amount of microwave is reflected back to the sample. The warm water load from microwave system is circulated through the cooling tower in order to reject heat to ambient. On the upstream side of the sample, an isolator is used to trap any microwave reflected from the sample to prevent the microwave from damaging the magnetron. The powers of incident, reflected and transmitted waves are measured by a wattmeter using a directional coupler (MICRO DENSHI., model DR-5000). Fiberoptic (LUXTRON Fluroptic Thermometer, model 790, accurate to ± 0.5 °C) is employed for temperature measurement. The fiberoptic probes are inserted into the sample, and situated on the XZ plane at Y = 25 mm. Due to the symmetrical condition, temperatures are measured for only one side of plane as illustrated in Fig. 2(a). An initial temperature of sample is 28 °C for all cases. Samples considered are water layer and saturated porous packed bed that composes of glass beads (diameter of 0.15 mm with a porosity of 0.385.) filled with water. Different dimensions of samples in the x-z direction are detailed in Fig. 2(b). A summary of the experimental procedure is depicted by Fig. 3. A sample container with a thickness of 0.75 mm is made from polypropylene which does not absorb microwaves. The samples will be heated by the microwave system that produces a monochromatic wave of TE10 mode having a frequency of 2.45 GHz. The dielectric properties for samples were measured at 28°C using a portable dielectric measurement (Network Analyzer) over a frequency band of 1.5GHz to 2.6GHz as shown in Fig. 4. The portable dielectric measurement kit allows for measurements of the complex permittivity over a wide range of solid, semi-solid, granular and liquid materials. It performs all of the necessary control functions, treatment of the microwave signals, calculation, data processing, and results representation. The software controls the microwave reflectometer to measure the complex reflection coefficient of the material under test (MUT). Then it detects the cavity resonant frequency and quality factor and converts the information into the complex permittivity of the MUT. Finally, the measurement results are displayed in a variety of graphical formats, or saved to disk. The dielectric properties of saturated porous packed bed that composes of glass beads filled with water which depends on temperature are depicted in Fig. 5 Table 1 and 2 summarize the dielectric properties of materials, i.e., glass beads and effective value of saturated porous packed bed. The penetration depths (skin depth) following Eq. (2) for each sample (water layer and saturated porous packed bed) at specified condition are summarized in table 1 and 2.

4. Results and Discussion

In this section, effects of various parameters on microwave-heating process are investigated. Effects of controlled parameters include microwave power, dielectric properties of sample, dimension and location of sample, on which the following subsections discuss.

4.1 Effects of power of microwave

Water which is the material examined is heated. The time evolution of temperature rise at the center point inside the water is shown in figure 6 with different values of power input. It is found that power significantly influences the rate of temperature rise. Greater power provides greater heat generation rate inside the medium, thereby increasing the rate of temperature rise. To understand further the power effects, table 3 and 4 include microwave power that goes towards (fwd) and comes out of (rev) water. The microwave powers of 300 W and 800 W are shown in table 3 and 4 respectively. In the case of higher power (800 W), more power energy is absorbed, and thereafter the absorbed energy is converted to more thermal energy, which increases the water temperature. The temperature profile along the x direction at the midlength in the y direction (Y = 25 mm) is shown in figure 7 for the heating time of 120 seconds. The same temperature data in figure 7 is also depicted in figure 8 as contour lines on the XZ plane in order to see the temperature distribution more clearly. Temperature is highest at the center location since the density of the electric field of the microwave field in the TE₁₀ mode is high around the center region in the wave

guide. The temperature is higher closer to the surface of water since water is a lossy dielectric material, which has a small penetration depth causing the field to decay rapidly. The penetration depth of water shown in table 1 is computed using equation (5) based on the dielectric properties of water [5]. The temperature profile at Z = 10 mm. in figure 7 is traced with respect to time and plotted in figure 9. It is clear that temperature rises with time. At each selected time, there appears the bulge shape along the centerline, suggesting that the lateral temperature gradient exists. The unstable condition causes flow motions induced by buoyancy force resulting convection mode of heat transfer. Temperature change along the z-direction at X = 55 mm and Y = 25 mm is measured and illustrated in figures 9 and 10 for microwave power of 300 W and 800 W respectively. In both cases, temperature is higher near surface. The case in which power of 800 W is used has greater rate of temperature rise, In addition the temperature is slightly more uniform than that for power 300 W due to greater rate of energy transfer per volume. Results presented in figure 10 are consistent to the results depicted in figure 7.

4.2 Effects of dimensions and location of material

The following discussions involve investigations of effects of dimensions of material and its location inside the wave guide on heating processes. Water in a container with different dimensions is heated by a microwave power of 300 W. Temperatures measured by fiberoptic are averaged and recorded. The resulting data is then plotted and shown in figure 11. The dimension sizes of container in the x, y and z directions are denoted by X, Y, Z respectively. It is found that the water that has smaller volume has higher rate change of temperature due larger heat generation rate per unit volume. However, the exception is observed. Although the water in a $110(X)\times30(Z)\times50(Y)$ mm³ container has larger volume than that in a 55×50×50 mm³ container, the water with the larger volume has greater rate of temperature rise. The reason behind this result is that the penetration depth of water that is greater than its thickness causes the interference of waves reflected from the interface of water and air at the lower side due to the difference of dielectric properties of water and air. Consequently, the reflection and transmission components at each interface contribute to the resonance of standing wave inside the water sample. Therefore the field distribution does not posses an exponential decay from the surface. In terms of location of sample, the sample which is water with 55mm × 30mm × 50mm in dimensions is placed in the waveguide at different locations as depicted in Fig. 12. After the heating time of 120 seconds, temperature is measured at X = 27.5 mm Y = 25 mm Z = 30 mm, and plotted with time in figure 13. It can be seen in this figure that the rate change of temperature is highest when location of the sample is shifted to 20 mm away of the

center, whereas the rate is lowest when the sample is located at the center. This is caused by stronger resonance effects that occur due to disorder wave reflections. Since sample has its length smaller than the waveguide width, waves reflect disorderly corresponding to a multimode of field pattern.

4.3 Effects of dielectric properties of material

Microwave-heating process within the saturated porous material is examined in this section. The sample used as the saturated porous material is the porous packed bed filled with uniform glass beads and water. Each glass bead is 0.15 mm in diameter. It can be observed in figures 14 and 15, which respectively present the line plots and contours that temperature is high around the bottom region in the packed bed. Due to differences in dielectric properties of the porous material and water, the present result is different than that found in the case of water. The dielectric properties of saturated packed bed are tabulated in table 2. It is clear that the porous packed bed has its penetration depth much larger than that of water shown previously in table 2. This porous bed which is considered a low lossy material in which the fields can penetrate much further, causing high temperature region at the bottom of the bed. This is confirmed by some microwave power that penetrates out of the bottom surface of the bed, as shown in table 4. In case of water shown in table 3, much less power goes through the bottom surface to air. Further, the temperature distribution of porous bed (figure 14) and water (figure 8) are compared. It is found that temperature in the XZ plane is more uniform in water than that in porous bed since more convection mechanism exists in water, while conduction is dominant in the porous bed due to minimal flow activities. To better understand the heat transfer mechanisms within the sample, the time evolution of temperature profile at Z = 10 mm. is plotted in figure 16. It is found that the range of temperature is substantially wider as compared to the case of water sample shown previously in figure 10. In this case, fluid motion is suppressed due to reduced permeability of porous bed. Consequently, the fluid is nearly stagnant indicating that conduction is a dominant mode of heat transfer.

5. Conclusions

The experimental analysis is presented in this paper, which describes many of important behaviors within dielectric materials during microwave heating. Based on the obtained results in the present study, findings can be summarized as follows:

1. Greater power provides greater heat generation rate inside the medium, according to the fact

- that the electromagnetic heat generation is proportional to the electric intensity to the power of two
- 2. The sample that has smaller volume has higher rate change of temperature due larger heat generation rate per unit volume. Sample with smaller thickness in the direction of the wave incident has higher rate of an increase in temperature. Within the smaller-thickness sample, the reflection and transmission components at each interface contribute to a stronger resonance of standing wave inside the sample.
- 3. Since the porous packed bed has its penetration depth much larger than that of water, the electromagnetic fields can penetrate much further, resulting in high temperature region at the bottom of the bed.
- 4. Convection due to buoyancy forced flows which is induced by lateral temperature gradient is considerable in water. However, in case of porous bed, conduction prevails due to minimal flow activities caused by the retarding effect within the bed.

References

- [1] A.C. Metaxas, R.J. Meridith, Industrial Microwave Heating, Peter Peregrinus, Ltd., London, 1983.
- [2] C. Saltiel, A. Datta, Heat and mass transfer in microwave processing, Adv. Heat Transfer 30(1997) 1-94.
- [3] K.G. Ayappa, S. Brandon, J.J. Derby, H.T. Davis, and E.A. Davis, Microwave driven convection in a square cavity, AIChE J. 31(5) (1994) 1268-1272.
- [4] J. Clemens, C. Saltiel, Numerical modeling of materials processing in microwave furnaces, Int. J. Heat and Mass Transfer 39 (8) (1996) 1665-1675.
- [5] D.C. Dibben, A.C. Metaxas, Frequency domain vs. Time domain finite element methods for calculation of fields in multimode cavities, IEEE Transaction on Magnetic 33(2) (1997) 1468-1471.
- [6] H. Zhao, I.W. Turner, The use of a coupled computational model for studying the microwave heating of wood, Appl. Math. Modeling 24 (2000) 183-197.
- [7] JR. Bows, ML. Patrick, R. Janes, A.C. Metaxas, et al., Microwave phase control heating, Int. Journal of Food Science and Technology 34 (1999) 295-304.
- [8] H. Zhao, I.W. Turner, G. Torgovnikov, An experimental and numerical investigation of the microwave heating of wood. J. Microwave Power and Electromagnetic Energy 33 (1998) 121-133.
- [9] J. Watanuki, Fundamental study of Microwave Heating with Rectangular Wave guide, M.S. Thesis (In Japanese), Nagaoka University of Technology, Japan, 1998.
- [10] Chatterjee, S., Basak, T., Das, S.K., Microwave driven convection in a rotating cylindrical cavity: A numerical study, Journal of Food Engineering 79 (4), 2007, pp. Page 48 of 62